



8-1996

# Design and Fabrication of a Mechanical Device for "in-situ" Measurement of Density of a Wood Particle Mat during Pressing

Estevao V.C.M. de Paula  
*University of Tennessee, Knoxville*

---

## Recommended Citation

de Paula, Estevao V.C.M., "Design and Fabrication of a Mechanical Device for "in-situ" Measurement of Density of a Wood Particle Mat during Pressing." PhD diss., University of Tennessee, 1996.  
[http://trace.tennessee.edu/utk\\_graddiss/4342](http://trace.tennessee.edu/utk_graddiss/4342)

This Dissertation is brought to you for free and open access by the Graduate School at Trace: Tennessee Research and Creative Exchange. It has been accepted for inclusion in Doctoral Dissertations by an authorized administrator of Trace: Tennessee Research and Creative Exchange. For more information, please contact [trace@utk.edu](mailto:trace@utk.edu).

To the Graduate Council:

I am submitting herewith a dissertation written by Estevao V.C.M. de Paula entitled "Design and Fabrication of a Mechanical Device for "in-situ" Measurement of Density of a Wood Particle Mat during Pressing." I have examined the final electronic copy of this dissertation for form and content and recommend that it be accepted in partial fulfillment of the requirements for the degree of Doctor of Philosophy, with a major in Engineering Science.

Robert D. vonBernuth, Major Professor

We have read this dissertation and recommend its acceptance:

Bobby L. Bledsoe, Fred D. Tompkins, Paul M. Winistorfer

Accepted for the Council:

Dixie L. Thompson

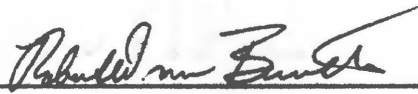
Vice Provost and Dean of the Graduate School

(Original signatures are on file with official student records.)

---

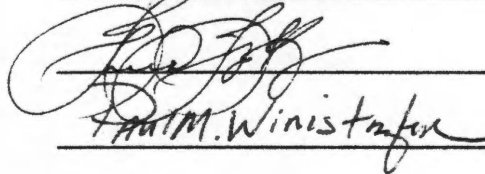
To the Graduate Council

I am submitting herewith a dissertation written by Estevao V. C. M. de Paula entitled " Design and Fabrication of a Mechanical Device for "in-situ" Measurement of Density of a Wood Particle Mat during Pressing." I have examined the final copy of this dissertation for form and content and recommend that it be accepted in partial fulfillment of the requirements for degree of Doctor of Philosophy, with a major in Agricultural Engineering.



Robert D. vonBernuth, Major Professor

We have read this dissertation  
and recommend its acceptance:



Accepted for the Council:



Associate Vice Chancellor  
and Dean of the Graduate School

**DESIGN AND FABRICATION OF A MECHANICAL DEVICE FOR  
"IN-SITU" MEASUREMENT OF DENSITY OF A WOOD  
PARTICLE MAT DURING PRESSING**

A Dissertation

Presented for the

Doctor of Philosophy

Degree

The University of Tennessee, Knoxville

Estevao V. C. M. de Paula

August 1992

## **DEDICATION**

**I dedicate this dissertation to my wife**

**Margaret de Paula**

**and my daughter**

**Juliana**

## ACKNOWLEDGMENTS

I wish to express my sincere gratitude to Dr. Bobby L. Bledsoe, my acting chair of committee, for his guidance during this work from its initial stages to the very last details. His dedication is gratefully acknowledged. Also, I would like to thank the other members of my doctoral committee, Drs. Paul M. Winistorfer, Robert vonBernuth and Fred D. Tompkins, for their time and comments in reviewing this dissertation. Dr. Paul M. Winistorfer gave an inordinate amount of his time through discussions and advice which proved particularly fruitful. I am also very grateful to Mr. W. Garner who constructed the device which is the centerpiece of this work and Mr. W. W. Moschler who prepared the samples and closely monitored the radiation tests. On the financial side I owe many thanks to people and Institutions. I would like to mention specifically the National Institute for Research in Amazon (INPA) and the Amazonian Technological Institute (UTAM), my primary supporters. I am also particularly thankful to Maria Tereza Cabral Dutra, a good friend, who made sure our bureaucratic problems were quickly and smoothly solved in Brazil. In a large time frame, I am deeply indebted to my parents Edgar and Helena for their support, dedication and orientation in my earlier years and to my parents-in-law Mario and Tereza who have always supported us in these difficult years away from home. Finally, I want to express my deepest gratitude to my wife Margaret and daughter Juliana. Their love, patience, encouragement and belief in my abilities made it come true.

## ABSTRACT

The objective of this research was to design, fabricate and evaluate a device for *in situ* measurement of horizontal density of a wood particle mat during pressing. Requirements of the device were to maintain selected relative fixed positions, with reference to the press opening distance, during press closure.

A mechanical device was designed to accommodate the requirements of the press environment, and to incorporate existing radiation based measurement equipment already in use in the laboratory. A system of stainless steel gears and racks was designed to maintain proportional velocity among three source and detector holders across the 24 inch opening of the existing hot press. Three individual positions selected for simultaneous radiation monitoring were 25%, 50% and 75% of mat height at any time during the press cycle. Aluminum yoke and source/detector holders were fabricated and attached to the press through a series of linear bearings. Aluminum plate stock was used to fabricate a frame to which all racks, gears and yokes were attached. A teflon insulating pad was placed between all surfaces of the mechanical device and the press to minimize heat transfer to the device.

After installation of the device on the press, an adjustment and calibration procedure was done to ensure positioning and collimation of the source and detector.

Evaluation of the performance of the device included employment of two

linear variable displacement transformers to monitor the source and detector positions during press closure. The average relative difference in position of the source and detector holders was 0.003 inches during evaluation of a normal press cycle.

An Americium<sup>241</sup> source, with a photon energy of 60 KeV, coupled to a sodium iodide crystal detector was used for initial measurements of density during pressing. Calibration samples (oak blocks) were used to determine the linear attenuation coefficient during experimentation. A constant linear attenuation coefficient of 0.21 cm<sup>2</sup>/g was found for different width calibration samples.

42 lb/ft<sup>3</sup> laboratory panels were manufactured for initial measurement of density during pressing. Mats were cut to 2, 4, 6, 8, and 12 inches in width to evaluate attenuation distance influence on density measurement. Plots were developed depicting density change with time, during the press cycle. These plots revealed changing density during pressing; most notable is the dynamic change in density after the press has reached final position. These are the first recorded *in situ* measurements of density of a wood particle mat during pressing.

The system of gears and racks provided an accurate method for maintaining desired positions of the radiation source and detector during pressing. The application of a radiation-based measurement technique to measuring density proved successful during initial experimentation.

## TABLE OF CONTENTS

Chapter	Page
1 INTRODUCTION	1
Background	1
Objective	3
Justification	3
2 LITERATURE REVIEW	5
Density distribution in wood-particle board	5
Process variable effects on density profile	6
Temperature and compaction pressure	7
Gas pressure	9
Moisture content	10
Press closing time	12
Theoretical density profile models	14
Properties related to density profile	16
Measurement of density	19
Measurement of density using gamma radiation	22
Moisture, temperature and adhesive effects on density measurement	25
3 DESIGN APPROACH AND RESULTING APPARATUS	30
Requirements of the device	30
General requirements	30

<b>Chapter</b>	<b>Page</b>
Specific requirements	31
Mechanism configuration	34
Definition of major components	40
<b>4 COMPONENT DESIGN AND FABRICATION</b>	<b>42</b>
Base plate and associated components	42
Source/detector alignment	43
Yoke-translation components	44
Speed multiplier mechanism	46
Gear housing	49
Platen drive rack components	53
<b>5 EVALUATION TESTS</b>	<b>55</b>
Installation of the device	55
Calibration of source and detector holding tubes initial vertical position	57
Measurement of accuracy and backlash Accuracy of the instruments	59
Tracking accuracy of the source and detector	64
Backlash of the drive train between yokes	67
Evaluation of density measurements during pressing Theoretical development and assumptions	71

Chapter	Page
System description	72
Calibration	73
In-situ measurements	74
Results and discussion	78
6 CONCLUSION	89
BIBLIOGRAPHY	91
VITA	96

**LIST OF TABLES**

<b>Table</b>	<b>Page</b>
4.1 Characteristics of speed multiplier gears.	46
5.1 Summary of regression analysis from data obtained in the first series of tests.	62
5.2 Average of deviation measured between L1 and estimate (first series).	63
5.3 Summary of regression analysis from data obtained in the second series of tests.	65
5.4 Average of deviation measured between L1 and estimate (second series).	66
5.5 Summary of the regression analysis from data obtained in the third series of tests.	69
5.6 Relationship between velocities of yoke 3 and yoke 1	70
5.7 Linear attenuation and mass attenuation of the calibrated sample.	75

## LIST OF FIGURES

Figure	Page
2.1 Schematic presentation of the density profile of a wood-particle panel through its thickness.	6
2.2 Schematic illustration of the relationship between pressure, closing time, and density distribution over the cross-section of medium density fiberboard ( Adapted from : Suchsland and Woodson 1975).	14
3.1 Initial (at start of pressing operation) positions of press, and desired position of three radiations sources and detectors for measuring instantaneous density "in-situ" of a wood particle mat during pressing.	32
3.2 Kinematics of rack-pinion device.	34
3.3 Front view (a) and side view (b) of press yoke-translation device for translocation of sources and detectors in fixed horizontal planes relative to the mat height.	38
3.4 Section A-A of the mechanical device.	39
3.5 Mechanical device on the press.	41
4.1 View of the linear bearings positioning yoke at two positions symmetrically placed on top of press.	43

Figure	Page
4.2 View of the detector/source attachment assembly.	45
4.3 Pictorial view of the speed multiplier mechanism.	47
4.4 View of gears of the speed multiplier mechanism.	48
4.5 Step-up gear, housing, shaft assembly.	50
4.6 Attachment of gear box 1 to yoke and rack.	51
4.7 Attachment of gear box 2 to yoke.	52
4.8 Primary drive components (right side shown, left side opposite)	54
5.1 Yoke displacement during press time.	60
5.2 Displacement yoke 1 and yoke 3 (press closing portion).	68
5.3 Schematic representation of the gamma densitometer apparatus. SC) press digital servo controller; PS) sample; L) LVDT; S) source; D) photoscintillation detector; E) Electronics for gamma detection; C) PC microcomputer.	73
5.4 Calibration test (four thicknesses of Oak).	76
5.5 Density during press cycle (sample:8 - width:2").	79
5.6 Density during press cycle (sample:9 - width:4").	80
5.7 Density during press cycle (sample:11 - width:6").	81
5.8 Density during press cycle (sample:12 - width:8").	82
5.9 Density during press cycle (sample:13 - width:12").	83

Figure	Page
5.10 Density during press cycle (sample: 8 - width:2"), smoothed plot.	84
5.11 Density during press cycle (sample: 9 - width:4"), smoothed plot.	85
5.12 Density during press cycle (sample:11 - width:6"), smoothed plot.	86
5.13 Density during press cycle (sample:12 - width:8"), smoothed plot.	87
5.14 Density during press cycle (sample:13 - width:12"), smoothed plot.	88

## **CHAPTER 1**

### **INTRODUCTION**

#### **BACKGROUND**

Wood-base composites continue to become an increasingly more important product segment of the wood industry. The developing trend for wood composites is toward increasing use of previously lesser used species, improved product performance through adhesive and process variable research, and product diversification. Molded products and combinations of wood and non-wood materials are also receiving considerable attention. Regardless of product diversification or improved product performance, the method of manufacture basically remains the same; products are pressed in a hot-press utilizing heat and pressure to catalyze the adhesive system and consolidate the loose mat or mold of wood material into a finished product.

The press environment and internal mat environment of these wood-composites during manufacture influences resulting product properties. Of particular interest is the influence of the mat environment on density and density variation of the finished product. Density has a strong relationship with mechanical and physical properties of these products and has been studied extensively for flat-pressed panel products (Strickler, 1959; Suchsland and Woodson, 1975; Woodson, 1976; Winistorfer

et al., 1986; and Laufenberg, 1986). While mat density can be monitored perpendicular to the plane of thickness during the lay-up of wood particles, no method currently exists to monitor density of the mat parallel to the plane of thickness during pressing; i. e., horizontal layer(s) within the mat. A method to monitor the density of the mat during manufacture would increase our understanding of mat dynamics during pressing as influenced by the press and mat environments. Developing such a method would lead to a more thorough understanding of manufacturing variables and their influence on finished panel properties, allowing some control over the "design during pressing" of such products.

Previously, information on density and density variation within a mat has been collected by empirical sampling from the panel after pressing. Boards have been sectioned and density has been measured via destructive (gravimetric) or non-destructive (x-ray or gamma radiation) methods. While post-manufacture determination of density is quite useful, a method to measure density *in-situ* during pressing would substantially increase our understanding of product manufacture and performance.

This research describes the application of radiation attenuation as a method for measuring the density of a wood mat during pressing. No previous method of *in-situ* monitoring of density during pressing has been reported.

## OBJECTIVE

The objective of this research was to design, construct and test a device for monitoring *in-situ* the dynamic density of a wood particle mat during pressing.

## JUSTIFICATION

The development of the density profile in a wood particle mat as influenced by variables controlled during the process of manufacture has been described by several researchers (Strickler, 1959; Suchsland, 1962; Winistorfer et al., 1986; Harlless et al., 1989; Humphrey, 1990 and; Kamke and Wolcot, 1991). Theoretical considerations about the phenomena that occur in the mat have lead to conclusions about the density variation of a wood particle mat and the variables that have the most influence on finished board properties. The complex physical-chemical interactions that occur in the mat during pressing have impeded a thorough understanding of density variation in the horizontal planes within the mat; a system for direct measurement of density in a horizontal plane(s) is needed. Therefore, a method for measuring *in-situ* density of a wood particle mat during pressing would augment our understanding of the theories regarding product manufacture.

Successful completion of this project would improve our understanding of product manufacture and performance, specifically, addressing the following:

1 - Provides a direct method to measure real-time density in a horizontal plane of a wood particle mat during manufacture.

2 - Introduces a new application of a well-known, non destructive method that allows the development of a feedback mechanism to control the manufacturing process and improve technological qualities of wood particle panel products.

3 - Enables the evaluation of theories already developed or generates new theories about the effect of the variables utilized for wood particle panel manufacturing.

4 - Introduces the possibility of using a variety of scanning methods or techniques to produce different images for different purpose. For instance, infrared images for tracking heat movement in the mat.

## **CHAPTER 2**

### **LITERATURE REVIEW**

#### **DENSITY DISTRIBUTION IN WOOD-PARTICLE BOARD**

Density is one of the most important characteristics of wood and wood products. Physical, mechanical and technological properties of wood and wood products can be estimated based on density. The density distribution in a board is a result of a complex interaction among external effects (heat and pressure) and rheological properties of the wood during the process of manufacture. According to Suchsland (1962), the density profile is caused by the mutual effect of the hot platens, temperature, and furnish (wood flakes) moisture content on the compression strength of the wood in the mat during pressing. During manufacture, heat is applied to primarily cure the adhesive, but also aids in improving the contact between flakes by plasticizing the wood material through plastic flow of the lignin. Heat being transferred from the platen to the face of the mat causes movement of water from the face to the core of the mat. Therefore, during manufacture the mat has different moisture contents and temperatures throughout its thickness. Layers in the mat are therefore compressed at different levels under the same external pressure because the stress-strain relationship of the wood in planes perpendicular to the fiber changes according to mat moisture content and temperature. As a

result, the density distribution within a hot-pressed panel is not constant because of this differential layer compression. Figure 2.1 shows the density profile of a typical wood-particle panel through its thickness.

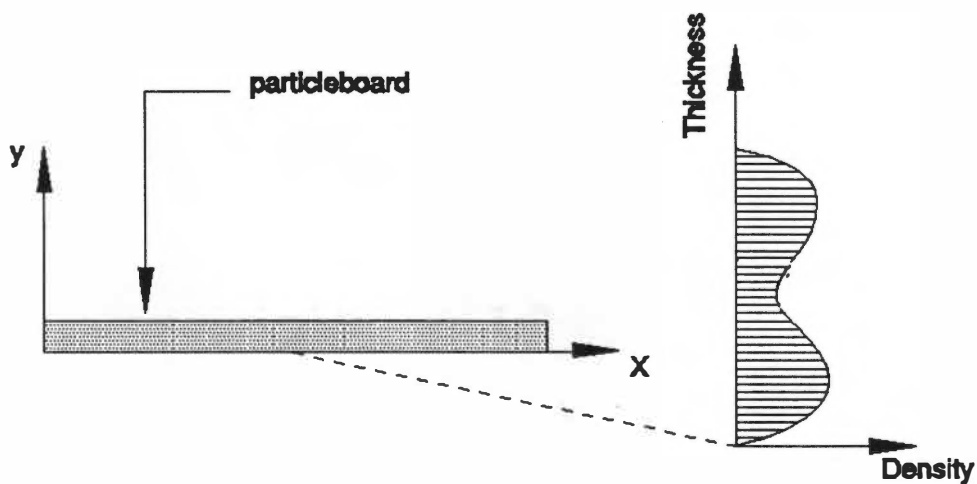


Figure 2. 1 - Schematic presentation of the density profile of a wood-particle panel through its thickness

### **PROCESS VARIABLE EFFECTS ON DENSITY PROFILE**

There is a complex interaction among process variables that has important effects on the formation of the density profile within the mat during pressing. The formation of density profile is influenced by the following process variables:

1-temperature and compaction pressure

2-gas pressure

3-moisture content

4-press closing time.

### **Temperature and compaction pressure**

Temperature and compaction pressure are external factors that contribute significantly to the manufacture of wood panel products. These two factors plus initial moisture content and geometry of the flakes generate a complex environment in a board during manufacture.

Heat flows into the mat by conduction, convection and radiation (Strickler 1959). Strickler pointed out that conduction can be negligible because wood is a poor conductor. Transference of heat into the mat by radiation is not significant because the lack of sufficient void volume in the mat to allow a consistent process of radiation; convection is the main cause of the transference of heat into the mat. The phenomenon of heat convection in the mat is justified by the fact that the effect of moisture relative to heat penetration through the center of the board is more significant than the effect of pressure.

The effect of temperature, gas pressure and compaction within the face and core region of a flakeboard was studied by Kamke and Casey (1988). They measured the temperature of a flakeboard at the face and core during pressing. Results of their experiment indicated that the temperature in the mat does not

respond fast at the beginning of pressing because a minimum compaction of the mat is required for developing some resistance against gas flow into the mat. According to Kamke and Casey, the mat does not offer resistance to the flow of gases at the beginning of the process because the mat is highly permeable. Temperature of the mat is also dependent on the press closing time; quick mat temperature rise corresponds to fast press closing time. The densification of the mat reduces the void volume and heat by conduction becomes more significant than heat by convection; as a result, the rate of temperature rise at the core layer is increased. A high platen temperature increases the rate of temperature rise in the mat face but not in the mat core layers. In the core, the significant factor influencing heat transfer is moisture. At 15% initial moisture content, temperature of the core layers at the end of press time was almost the same among the samples studied, although the samples had been made under different conditions of press temperature and press closing time. At 6% initial moisture content, the core temperature presented different patterns than samples with 15 % initial moisture content: after 6 minutes of venting, core temperature can either increase to 190 °C or remain almost the same at 154 °C. The sensible heat transferred from the platen at 190 °C had not been consumed at low moisture content (Kamke and Wolcott, 1991). Kayihan and Johnson (1983), in their preliminary experiments aimed at understanding the movement of heat and moisture in wood composite materials during the pressing operation, observed an "unusual dip" in the core temperature when the mat is pressed for a long time. They credit the quick release of vapor as the cause of this " unusual dip " because the speed of

the movement of pressure, air and water vapor are controlled by the board permeability. At the beginning of pressing, temperature increases, the wood fiber plasticizes, and the mat permeability is reduced; as a result, the formed vapor is trapped in the core of the mat. With the mat being pressed for a long time, the amount of vapor increases until a pressure is reached which overcomes the resistance to flow-out and the temperature of the core drops with the liberation of the vapor.

### **Gas pressure**

Gas pressure generated during the manufacture of a board is caused by water vapor from wood cell walls and " a product of the condensation reaction of the phenolic adhesive " ( Kamke and Casey, 1988). They also pointed out that volatile extractives might contribute to the generation of gas pressure. In addition, Kamke and Casey concluded by applying the ideal gas law ( $PV = nRT$ ) to the experimental data that the moisture has a significant effect on the formation of the gas pressure in the mat. Two situations were studied: a)  $nR/V$  constant and  $P$  controlled by the change of temperature; b)  $RT/V$  constant and  $P$  controlled by the change in amount of water vapor,  $n$ . Comparing these two situations they found that the pressure due to the change in the amount of water is bigger than the resultant pressure due to the change in temperature. There was no substantial change in gas pressure until the mat had reached a certain compaction when the edge gave some resistance to gas flow. The formation of the density profile can be explained by the variation of the gas pressure during pressing (Kamke and Casey, 1988). For instance, a noticeable

peak in gas pressure at the end of final thickness position of the board was detected during the experiment. This peak was more pronounced for a fast press closing time and high moisture content because more air is trapped before reaching the final thickness position. When the maximum platen pressure is not reached but the final thickness is reached, some voids can remain open due to stress relaxation and the gas pressure will be reduced as a result of greater volume and more permeability. According to Kamke and Casey, gas pressure is an indication of void volume; therefore, a portion of the density gradient might be formed after the mat has reached its final thickness.

Internal stress relaxation, resin cure and densification of the mat can be affected by water vapor pressure gradients and resultant vapor flow (Humphrey, 1990). Bolton et al. (1989) pointed out the risk of board failure when the press is opened if there is a large difference in vapor pressure between the inside and the outside of the mat. In summary, temperature and gas pressure seem to be good indicators of the formation of the density gradient in a mat during the manufacturing of a board.

### **Moisture content**

The movement of moisture into the mat has a strong effect on the shape of the density profile. The path of the water into the mat is governed by the geometry of the flakes. According to Geimer (1975) moisture moves around the particles rather than through them. The effect of furnish moisture content and moisture

distribution on the density of a board was studied by Strickler (1959). He incorporated Douglas-fir furnish, three target densities, three moisture contents, six press cycles and two replications. Boards with non-uniform distribution of moisture in the mat were also studied. Strickler reported that moisture content and the distribution of the moisture within the mat govern and control the rate of heat penetration to the center of the board. The distribution of density through the thickness of a board, after pressing, is influenced by the moisture content of the mat. During pressing, moisture moves fast from the surface to the intermediate layers, but movement slows from the intermediate layer to the center layer because the temperature at the center layer is lower than at the surface. Therefore, the densification of the mat at the intermediate layers is greater than at the surface and center layer because the strength of the wood is inversely proportional to moisture; as a result the distribution of density through the thickness resembles the shape of "M."

Moisture movement in the mat was predicted by Kamke and Wolcott (1991). Their theoretical results indicated that panels made with initial moisture contents of 6 and 15%, with platen temperatures of 154 and 190 °C, resulted in similar movement of moisture in the mat during the initial minutes of pressing (1.5 min. and 2.5 min. for 6 and 15% of initial moisture content, respectively). Initially, the moisture content drops as the temperature rises; however, the liberation of bound water initiates water movement into the voids between flakes and the moisture content rebounds.

The effect of moisture as related to stress development and relaxation was discussed by Bolton et al. (1989). The residual stress is a function of the moisture content of the wood under load. For instance, the residual stress level decreases as the wood loses moisture; otherwise, the stress level increases. In addition, they pointed out that shrinkage and swelling of the wood increases and decreases the particle strain, respectively.

Humphrey (1990) pointed out that thermosetting adhesives are sensitive to temperature and moisture variation in the mat. He concluded that mats with low moisture content resulted in boards with high bond strength. In addition, he also verified that areas in the mat with high moisture content result in low bond strength.

### **Press closing time**

Press closing time was studied by Suchsland and Woodson (1975) and later by Smith (1982) as a variable which has a significant influence on the shape of the density profile. Suchsland and Woodson working with medium-density fiberboard pointed out that the effect of the press cycle on the distribution of density through the thickness of a board differs according to the press closing speed and level of pressure. They presented two hypothetical situations to obtain a board with a uniform distribution of density:

- a) a slow and long closing time with a low pressure.
- b) a fast or short closing time with a very high pressure.

Suchsland and Woodson studied a range of conditions between both situations

(a) and (b). They studied eight series of mats. Mats of the series A, B, and C were prepressed at a pressure of 60 psi, D was prepressed at 650 psi; mats of series E and F consisted of three layers and were prepressed at different pressures before being assembled. Boards of the series G were compressed to the stop without being heated; after stopping, the pressure was reduced and heat was applied until the temperature reached 285 °F. Series H was a commercial board cured with high-frequency. The results of this experiment indicate that the contrast of density increases at high pressure, although the highest pressure did not result in the highest density in the face. Mats pressed (series G) without being heated had an almost uniform density distribution. The density profile obtained by prepressing the core and the face at different pressure (E and F) resulted in a profile similar to boards in which the core and face were pressed with equal pressure (Figure 2.2).

Smith (1982) working with waferboard noted that the shape of the density profile depends on the rate of the press closing time. A short rate of press closing time causes a formation of the density profile in the shape of "U". The shape of the density profile changes from "U" to "M" with an increase in press closing time. The gradient of temperature between the surface and core are too high if the press closing time is fast; as a result, the surface of the mat will be more compressed than the core of the mat. The effect of press closing time was also pointed out by Davis (1989) working with a mixed hardwood flakeboard. He utilized a direct-scanning gamma densitometer to measure the vertical density profile of the sample and took twenty incremental measurements through the thickness of the sample. The thickness

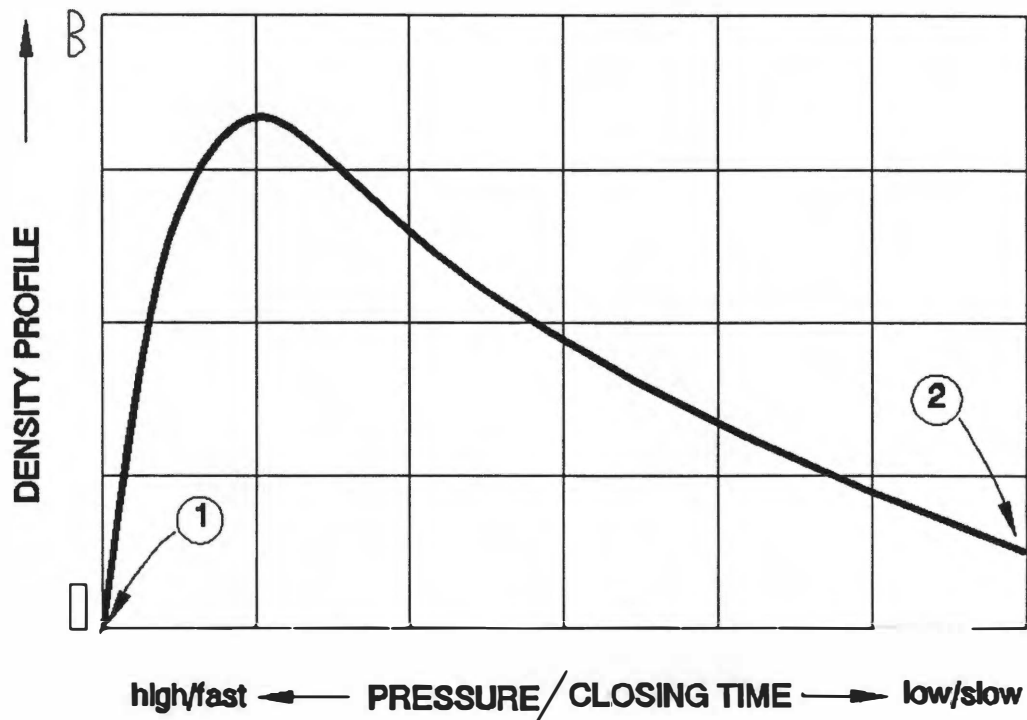


Figure 2.2 - Schematic illustration of the relationship between pressure, closing time, and density distribution over the cross-section of medium density fiberboard ( Adapted from: Suchsland and Woodson 1975).

of the sample was divided into five regions and the mean density value for each region was determined. The experimental results lead Davis to conclude that the density profile was strongly affected by press closing time.

### THEORETICAL DENSITY PROFILE MODELS

Several researchers have estimated the internal conditions in the mat based on existing mathematical models relevant to the internal environment of solid wood and assumptions based on the phenomenon of heat and mass transfer. Humphrey

(1990) developed a mathematical model which describes the relationship between the adhesive response and the environment in the mat during the manufacture of a board. The model was applied to a panel manufactured at the following conditions: 160 °C, 650 Kg/m<sup>3</sup>, 15 mm thick, Douglas-fir furnish, spray-dried powdered phenolic resin and initial mat moisture content of 11 %. His model showed that the maximum mat moisture content approaches 20 % in the core and about 6 % in the face of the board.

Kamke and Wolcott (1991) developed a model to estimate the gas phase composition of a mat during the manufacture of a board. The model is based on the Hailwood-Horrobin equation which is used to find the equilibrium moisture content of solid wood as a function of relative vapor pressure and numbers of hydrates.

Simpson (1973) studied seven analytical expressions which relate equilibrium moisture content to relative humidity and found that the best-fit model was the Hailwood-Horrobin model. Using the Hailwood-Horrobin equation and assuming that the mat leaks continuously through the edges, Kamke and Wolcott derived an equation as a function of measuring the temperature and gas pressure of the board during manufacture. Relative vapor pressure, equilibrium moisture content and average flake temperature were the variables included in this model. Temperature and gas pressure were measured experimentally to obtain the composition of the gas phase during the pressing process. Some interesting results were presented; equilibrium moisture content drops rapidly as the temperature increases. In the core, the relative vapor pressure and moisture content increase because the bound

water in the wood evaporates and moves into the void space between flakes. When venting begins, there is a dissipation of water vapor and as a result equilibrium moisture content is a function of the amount of water remaining in the wood.

Harless et al. (1989) developed a computer simulation to predict the density profile which considers the physical processes which occur within a wood mat during pressing. The model requires information about initial mat temperature, press temperature, open and close press times and target board density. The model presents graphical display of the density profile, represented by layer-density of a board at the end of a simulated press cycle. A one-dimensional model to describe the heat transfer from the platen to the mat was considered, and an expanded form of the heat conduction between platens derived by Siau (1986) was utilized. However, the model excludes the effect of the resin cure and plasticization which reduces the density of the face layer just below the mat surface. The effect of the plasticization and relaxation of individual particles and the changes that might occur in the density profile after the press has reached final position were also disregarded in this model.

### **PROPERTIES RELATED TO DENSITY PROFILE**

Modulus of elasticity (MOE) and modulus of rupture (MOR) in bending have a strong relationship to the density profile of flat pressed panels. Therefore, the mechanical properties of a board may be influenced during the manufacture of the

board. The effect of the density distribution through the thickness of a board on **MOE** and **MOR** was pointed out by Woodson (1976). Woodson compared two sets of boards; the first set made from three different species of wood (sweetgum, Southern red oak and hickory), two thickness (3/4 and 3/8 inch), two levels of pressure (240 and 800 psi), three press cycles (7, 8, 9 minutes) and the second set with a uniform distribution of density through the thickness of the board. The uniform density distribution was obtained by pressing the mat to stops in a cool press and keeping the mat under pressure until the platen temperature reached 285 °F. Woodson concluded that boards with a high gradient of density between the surface and center layer had a **MOE** value 30 to 50 percent greater than boards with a uniform density distribution. He also pointed out that a uniform density distribution was good for machining characteristics and internal bond although a uniform density profile resulted in the lowest bending characteristics during the experiment.

Strickler (1959), working with press cycles from 0 to 12 minutes, found that **MOR** decreases as press cycle increased; the difference in the density between the surface layer and center layer increases as press cycle increases. Therefore, **MOR** decreases as the density variation between layers increases. In addition, Strickler concluded that the relationship between **MOR** and surface layer density changes according to the press cycle. **MOR** for press cycles between 0 and 2 minutes was different from **MOR** for press cycles between 2 and 12 minutes; **MOR** increased for cycles between 0 and 2 minutes and decreased for cycles between 2 and 12 minutes. According to Strickler, the effect of stress relaxation after the press is opened results

in poor bonding of surface flakes because the resin was not yet polymerized at 2 minutes into the cycle, although high surface density remains. Steiner et al. (1978) pointed out the importance of the X-ray densitometer evaluation method for improving mill waferboard properties. Working with two sets of samples, Steiner reported improvement of 10 and 25 percent for internal bond (IB) and MOR, respectively, by changing the density profile of waferboard for more symmetric density distribution, although all samples presented similarities in average density.

MOE can be a good indicator of the variation of density between layers. Suchsland and Woodson (1975) pointed out that stiffness of a medium density board is independent of species, fiber geometry, specific gravity and glue condition. In his paper on the process and design for optimization of composite wood structural components, Laufenberg (1986) suggests that one method to improve the flexural stiffness and strength of the board is to control the variation in density through the panel thickness; however, this improvement might decrease the internal bond and interlaminar shear strength.

The relationship of the density profile to thickness swell (TS) and internal bond (IB) was studied by Davis (1989). Thickness swell increased as the difference in density between horizontal regions increased. IB also was responsive to the density profile; IB increased as the difference in density increased. In addition, Davis concluded that the core density strongly influences IB.

## MEASUREMENT OF DENSITY

The density profile can be measured by the conventional gravimetric method or by recently described radiation methods (Loos 1965; Laufenberg 1984; Winistorfer et al. 1986). The radiation method for measuring density of wood is based on the attenuation of the intensity of radiation emitted through the sample. The source used is dependent upon to the type and thickness of the material to be measured. Alpha, Beta, Gamma (Loos 1965) and X-ray are the radiation sources most used for measuring density or moisture of a wood sample. Alpha and Beta sources are restricted in use because of the limitation to a thickness of 2 cm (wood density of 0.5 g/cm<sup>3</sup>). Gamma rays are effective up to 40 cm thickness of wood at a density of 0.5 g/cm<sup>3</sup> according to Loos.

A direct-scanning densitometer system using X-ray is discussed by Cown and Clement (1983). They used an Fe-55 source emitting energy of 6 KeV. One of the advantages of X-ray over the other radiation sources is the possibility of using a variable level of energy. The main disadvantage of the X-ray is its high cost and the X-ray intensity is never constant, although the variation of the intensity can be negligible to a accumulative detector (Liebhafsky et al., 1960). Energy of the source is considered one of the most important operational factors of the radiation technique. There is a level of energy which the absorber or some element of the absorber does not attenuate. For instance, X-rays began to be utilized for measuring variation of density within a board after the advent of the "soft-radiation" by using

low voltage and enough radiation to verify the density (Near, 1968). Liu et al. (1988) determined the relationship between attenuated radiation and radiation not attenuated ( $I/I_0$ ) at different levels of energy, using ponderosa pine, 1 mm-thick. The energy ranged from 3.7 to 60 KeV and they found that the optimal X-ray energy for pine was 5.377 KeV. Their conclusion was based on the fact that energies of 10 KeV and over, as well as low energy (3.7 KeV), do not show the variation of the relationship between  $I/I_0$  relative to the function of the intensity of the attenuated radiation. In addition, they applied the same procedure and concluded that the optimal energy X-ray for nine species of wood ranged from 5.127 KeV (Scots pine) to 5.690 KeV (shore pine). As a conclusion, they concluded that the measurement of density by the radiation method is accurate only if the radiation energy used is close to the optimal energy.

The detector is a device used to catch the emission of radioactive substance. Geiger-Muller and scintillation counters are the most common detectors used for wood density measurement (Loos, 1965). According to Loos, the response of the Geiger-Muller to the 10,000 counts per minute is not linear and its efficiency for counting gamma radiation is only 1 %. The electric impulse generated by the scintillation counter is proportional to the energy of the radiation absorbed by the crystal. Loos suggested that scintillation detectors are superior to Geiger-Muller detectors. Liebhasfky et al. (1960) pointed out that the Geiger counters require frequent calibration if used to detect million counts per second and they therefore advise the use of proportional counters. Although Scintillation detectors are more

complicated and fragile than Geiger-Muller detectors, they are the most used for measurements with wood.

Count rate is a measure of radiation received by the detector during a desired time interval. A significant number of counts must be detected in a finite time (minutes to seconds) to obtain desirable confidence limits, as the count rate is expressed by the Poisson distribution. The count-rate meter is an instrument designed to measure a signal from the detector (Lapp and Andrews, 1949). The count-rate meter accumulates the pulses received by the detector during a time interval and gives the average count rate in this interval of time. A minimum interval between two consecutive recorded count rates is known as resolving time (Goldanskii, 1962).

The determination of density by radiation techniques is based on the attenuated count rate ( $I$ ) recorded from the count rate meter. Equation (2.1) show the relationship between count rate before and after passing through the sample .

$$I = I_0 * e^{-\mu_1 * t} \quad (2.1)$$

where

$I$  = intensity of the radiation beam after passing through the material

$I_0$  = intensity of the radiation beam before passing through the material

$t$  = sample absorbed thickness

$\mu_1$  = linear attenuation coefficient

Equation (2.1) can also be written:

$$\ln\left(\frac{I}{I_0}\right) = -\mu_l * t \quad (2.2)$$

The linear attenuation coefficient can be determined experimentally by finding the relationship between relative intensity (logarithmic scale) and thickness of the absorber.

The linear attenuation coefficient changes with the density of the absorber although the absorber material is the same (Liu et al., 1988). Linear coefficient attenuation is a product of mass attenuation coefficient and density of the absorber.

$$\mu_l = \mu_m * \rho \quad (2.3)$$

Density of the absorber can be determined by substituting equation 2.3 into the equation 2.2.

$$\rho = -\frac{1}{\mu_m t} \ln\left(\frac{I}{I_0}\right) \quad (2.4)$$

## MEASUREMENT OF DENSITY USING GAMMA RADIATION

The relationship of wood density, with a given moisture content, as a function of gamma rays absorbed, was studied by Lakatos 1956 (Loos, 1961). Loos, studying the sensitivity of monoenergetic gamma ray attenuation on the measurement of the gross density variation in wood, concluded that there is a high degree of accuracy for measurement of specific gravity by gamma radiation. His conclusion is based on the comparison between the linear attenuation coefficient ( $0.095 \text{ cm}^{-1}$ ) for sugar pine

determined by Parish (1958) and the linear attenuation coefficient ( $0.080 \text{ cm}^{-1}$ ) for yellow-poplar. Since the specific gravity of these two species and the source energy was the same (47 Kev), Loos concluded that the comparison is a good indicator of accuracy of the gamma radiation method for the determination of the mass attenuation. In addition, Loos presented a regression analysis between a calculated specific gravity from the linear attenuation coefficient and a measured specific gravity which shows accurate results for two different moisture contents ( 9 and 18 percent).

Laufenberg (1986) evaluated the method of determination of the mass attenuation of two species (red oak, douglas-fir) using gamma radiation by comparing the experimental results with theoretical results. The theoretical results were determined as a function of the primary elements of the wood. The comparison leads to a conclusion that there is no significant difference between the density of wood determined experimentally and theoretically. In addition, Laufenberg pointed out that one of the problems for the application of the density measurement technique is the measurement of the density near the face of the sample. The slit width utilized in his experiment produced poor resolution near the face; however, a smaller slit would have required a longer counting time for each sample to obtain the same precision as the slit utilized in his experiment. The problem of measuring near the face of the board is also pointed out by Winistorfer et al. (1986). In addition, they concluded that any misalignment among source, sample and detector causes a " spreading of the apparent edges of the sample."

Later, Moschler and Winistorfer (1990) suggested the sample be placed between material with density approximately equal to the density of the sample surface (face) to reduce the error of measuring near the face.

Moschler and Dougal (1988) presented a method of calibration for a direct scanning instrument. Thirteen wood blocks of different species, two energy sources ( $\text{Fe}^{55}$  and  $\text{Am}^{241}$ ) and two moisture content levels were studied. The regression analysis between linear attenuation coefficients and density of the wood indicated a correlation coefficient of about 0.99 for different energy sources and different moisture contents. The wood mass attenuation was determined by the parameters of the regression analysis. The difference between the wood mass attenuation coefficient obtained by Moschler and Dougal and that reported in the literature was less than four percent. As a result, they concluded that their calibration procedure was accurate, although their accuracy could have been improved by considering extractive content, level of ash, orientation of the sample and moisture content of the wood.

The limitations of direct scanning radiation densitometry using a gamma ray source is discussed by Moschler and Winistorfer (1990). They presented an equation to determine the error caused by the aperture area (slit) of a gamma densitometer. According to their numerical example, the error can reach up to 40 % if material with two different specific gravities (0.9 and 0.2) is detected in the same aperture. So, direct scanning radiation densitometry used on wood with an abrupt springwood and summerwood transition or ring porous hardwood, increases the probability of

aperture error. However, the reduction of the aperture size will reduce the count rate and consequently the precision for  $I$  and  $I_0$ . A large aperture size is recommended by Moschler and Winistorfer for use in the densitometry of panel and board products because of the thickness and relative high density of board samples and the possibility of using this technique as part of the production process; a large aperture would ensure adequate count rates in a short time which could be used for process control.

A mathematical model was suggested by Ferrand (1989) to establish a curve to account for variation in wood density and a function or "anatomy" function to describe a density model for wood. According to Ferrand, the main problem is the slit dimension of the microdensitometer in reference to the anatomical characteristics of wood. i.e., vessel lumen diameter and other anatomical features.

## **MOISTURE, TEMPERATURE AND ADHESIVE EFFECTS ON DENSITY MEASUREMENT**

Moisture and temperature change in the mat during the process of manufacturing a board. There is limited information about the effect of these variables on the measurement of density using gamma radiation. Moisture content of wood has been determined using gamma radiation. Loos (1965) presented several works that had been done to find moisture content of wood using nuclear radiation techniques. Loos (1961) also studied the relation between the linear absorption

coefficient and moisture content in wood. He applied gamma radiation using a source of lead<sup>210</sup> ( $P_b^{210}$ ) and a primary energy peak of 47 Kev. The samples studied were 6 cm thick yellow-poplar and their specific gravity was determined at green volume and oven-dry weight. Samples were conditioned to moisture contents of 0, 9, 18 percent and saturated. Through the experiments developed a mathematical model for estimating the variation of the linear absorption coefficient relative to density of the wood and its moisture content. There are five terms in the mathematical model; the first term is the ordinate intercept; the second term is the effect of the density on the measurement of the linear attenuation; the third term is the effect of the moisture content of the sample on the measurement of the linear attenuation and the fourth and fifth terms are power terms (square and cubic) on the moisture content. According to Loos, preliminary plots had shown that moisture content has a non-linear effect on the linear attenuation coefficient (from overdry to fiber saturation). He also concluded that there is no interaction effect between density and moisture content on the linear attenuation coefficient (from dry to fiber saturation) and stated " gamma ray absorption is proportional to percent moisture content ". Loos also introduced a mathematical model for moisture content above the fiber saturation point and concluded that there is interaction between density and moisture content above fiber saturation.

The effect of moisture content on X-ray attenuation is referred to by Hoag and Krahmer (1990). They cited Phillips works which had concluded that a variation of 10 % in sample moisture content would result in 0.37 % change in attenuation.

Hoag and Kramer also did experiments on the influence of moisture on X-ray attenuation by using Douglas-fir samples at different moisture contents. They found that there is a positive correlation ( $R\text{-square}=0.99$ ) between linear attenuation coefficient and moisture content in the range of 0 to 35 percent. They pointed out that the error in density is  $0.006 \text{ g/cm}^3$  for a difference of 1 percent in moisture content of the sample.

The effect of moisture content on the mass attenuation coefficient determined by using gamma radiation was described by Moschler and Dougal (1988). They scanned blocks of 12 different species of wood with two different sources ( $\text{Am}^{241}$  and  $\text{Fe}^{95}$ ). The difference of mass attenuation detected from boards with 8 percent and 0 percent moisture was only 3 % for both sources of energy. They recommend the operation of such a direct scanning system at room conditions because the effect of moisture is very small.

Ten percent moisture content could result in an underestimate of 1.0 % of density of an oak board by using gamma radiation at 60 KeV (Laufenberg, 1986). This error is caused by the difference between mass attenuation of the wood (0.186) and mass attenuation of the water (0.196). In addition, Laufenberg reported that the measurement of density by gamma radiation in an environment which results in 12 percent or less equilibrium moisture content of a board is less than 1 percent.

Temperature has not been reported as a factor which affects the mass attenuation coefficient measured by gamma radiation. However, temperatures above  $100^{\circ}\text{F}$  might have some effects on the detector because the circuit of the detector

usually works under electronic levels of energy up to a temperature of 100 °F.

Adhesive and its influence on the mass attenuation by using gamma radiation was studied by Laufenberg (1986). His experiment indicated that density is underestimated 0.4 percent for an oak board with 9 percent urea resin, and underestimated 0.1 percent for oak boards with 5 percent phenol resin. Resin usage in practice is much less than 9%; estimates for density are likely less influenced by the adhesive level now used in most mills.

Species of wood has no effect on the determination of density using gamma radiation (Laufenberg, 1986). Red oak and Douglas-fir had the same value of mass attenuation (0.183) in his experiment. On the other hand, Moschler and Dougal found that the use of different species of wood can be a source of error in determining wood density because the variation of mass attenuation among species. The error increased with the use of the  $\text{Fe}^{55}$  source because " some trace elements have a large elemental mass attenuation coefficient in this energy range ( 5-9 KeV ) and subsequently anomalous density readings result". Four different species of wood (balsa, birch, maple and rosewood) were utilized by Hoag and Mckimmy (1988) during their experiment with x-ray densitometry. The difference between density obtained by X-ray and gravimetric methods ranged from 0.8 to 3.6 percent for three of the species studied; however, balsa resulted in a difference of 35 percent. The effect of this difference was attributed to the 60 Hz noise caused by the self-rectified x-ray tube; although of small magnitude, the effect of noise is large for a low density wood. The level of inorganic matter in the wood can affect the

determination of density by gamma radiation (Laufenberg, 1986; Moschler and Dougal, 1988). The effect of ash on wood mass attenuation was described by Liu et al. (1988). They applied different levels of X-ray energy to spruce heartwood and plotted a graph of the ratio of the mass attenuation coefficient of ash element against different energies. The maximum contribution of the ash on the mass attenuation was 3.4 percent at an energy level of  $11 \pm 1$  KeV and of 1 % for soft energy. In addition, Liu et al. concluded that oxygen and carbon strongly effected the X-ray attenuation in wood.

## **CHAPTER 3**

### **DESIGN APPROACH AND RESULTING APPARATUS**

A method to monitor changes in the mat density profile during pressing has been noticeably absent from previous work relating to wood particleboard. The primary focus of this research was to develop a workable method to measure dynamically the changing density profile during the pressing operation. Thus a main thrust of this work was to design a mechanical device to enable measurement of mat density through predetermined horizontal layers within the mat using gamma radiation. The radiation source and detector must move with the constantly changing vertical position of the chosen horizontal layer of fibers as the mat is compressed to final thickness.

### **REQUIREMENTS OF THE DEVICE**

#### **General requirements**

The design of the mechanism to monitor "in-situ" the instantaneous density of a wood-particle mat during the pressing process must take into consideration the following requirements:

- a) The dynamic manufacturing process of wood-particle board, brought about

by the press platen moving at a certain speed, requires that the plane of measurement move in some proportion to the thickness of the mat during the pressing operation.

b) Source and detector must be in alignment relative to a specific layer (percent of thickness) within the mat section at which the density profile is to be continuously measured. For example, if the layer at the exact center of the mat thickness is to be continuously monitored for density while the mat is being compressed from 152 mm (6 inches) to 13 mm (0.5 inches) thickness, then the radiation source and detector must track exactly the center plane of the mat.

c) The operational condition of the press must not jeopardize the accuracy of the measurement. Therefore, the mechanism must perform in an environment with temperatures up to 204 °C (400 °F).

### **Specific requirements**

The horizontal planes desired for dynamic monitoring of density of the mat during the pressing operation were the mid plane, quarter plane, and three quarter plane of the mat thickness (figure 3.1).

Since the lower platen of the press moves relative to the upper fixed platen, the heated lower surface of the upper platen is taken as the reference plane. Relative to this reference plane, if the maximum press opening is  $X$ , then the thickness of the mat being pressed at any time ( $t$ ), after start, with the upward velocity of the lower platen being  $V$ , is:

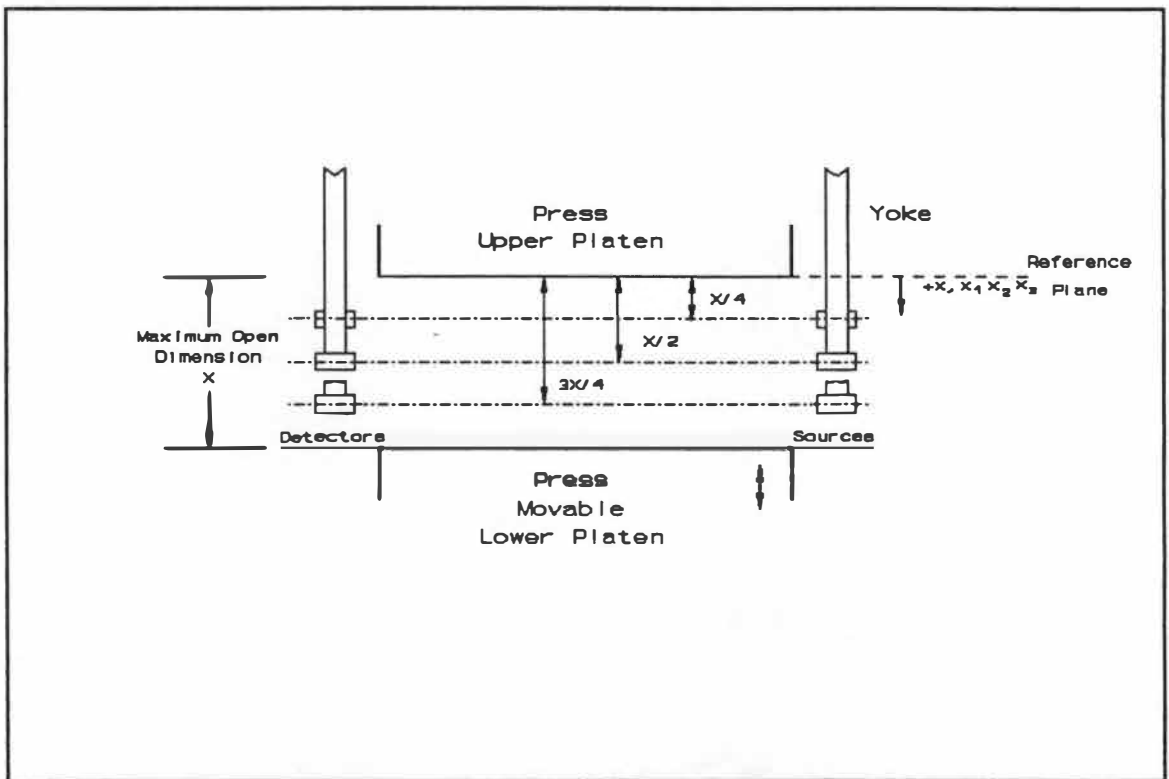


Figure 3.1 - Initial (at start of pressing operation) positions of press, and desired positioning of three radiation sources and detectors for measuring instantaneous density "in-situ" of a wood particle mat during pressing.

$$x(t) = X - Vt \quad (3.1)$$

One radiation source and detector could be positioned at the exact center, vertically, of the distance between the press platen horizontal surfaces when maximum open. If this source and detector are moved vertically at half the velocity of the lower platen of the press, the source and detector will always be positioned at the midpoint of the mat thickness.

$$x_1(t) = \frac{X}{2} - \left(\frac{V}{2}\right)t \quad (3.2)$$

Similarly a second radiation source and detector could be positioned initially at the

quarter point of the maximum press opening relative to the reference surface. And a third source and detector could be positioned at the three quarter point of the maximum press opening. If these added sets of sources and detectors are moved at one-fourth and three-fourths the velocity of the lower platen of the press, respectively, then the second set will always be positioned at the quarter point of the mat thickness and the third set at the three-quarter point.

$$x_2(t) = \frac{X}{4} - \left(\frac{V}{4}\right)t \quad (3.3)$$

$$x_3(t) = \left(\frac{3}{4}\right)X - \left(\frac{3}{4}\right)Vt \quad (3.4)$$

In summary, the four equations defining mat thickness,  $x$ , and source-detector positions, all relative to the reference plane, and all as a function of the lower platen velocity and time after start of pressing are:

$$x(t) = X - Vt \quad (3.1) \text{ Mat thickness}$$

$$x_1(t) = \frac{X}{2} - \frac{V}{2}t \quad (3.2) \text{ Position of mid plane}$$

$$x_2(t) = \frac{X}{4} - \frac{V}{4}t \quad (3.3) \text{ Position of quarter plane}$$

$$x_3(t) = \frac{3}{4}X - \frac{3}{4}Vt \quad (3.4) \text{ Position of three quarter plane}$$

## MECHANISM CONFIGURATION

To implement motion equations (3.1) through (3.4) precisely, without no slip, a rack and pinion type mechanism was chosen. For the mid plane positioning variable,  $x_1$ , the drive racks are fixed to the lower platen of the press. These drive pinions whose shafts were fixed to a movable yoke supporting the mid-plane radiation source and detector. The drive pinions also mesh with racks identical to the drive racks but fixed to the upper platen of the press (figure 3.2). With such an arrangement, the velocity of the yoke supporting the mid plane radiation source and detector can be determined in terms of the lower platen velocity as follows.

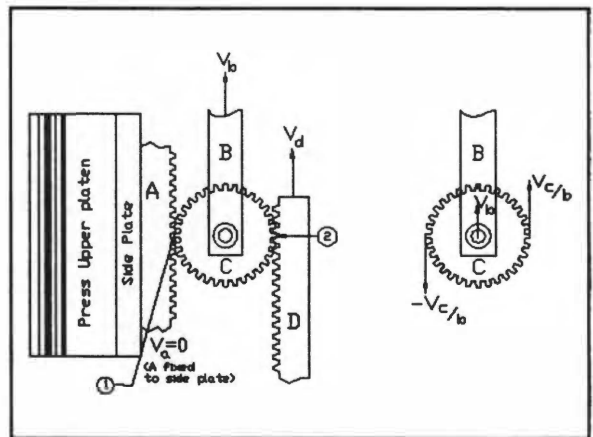


Figure 3.2 - Kinematics of rack-pinion drive.

As seen in figure 3.2, the pinion C rotates about its axis (center of the shaft) fastened to yoke B. At the point of engagement with the fixed rack A, the absolute velocity of that point of pinion C must be zero, the same as the fixed rack (reference body). At the point of the contact with the drive rack D the absolute velocity of the point C must be the same as that of the upward moving rack, V. Designate point 1 as the contact point with the fixed rack, and point 2 as the point of contact with the driving rack D. Then

$$V_{c_1} = -V_{c/b} + V_b = 0 \quad (3.5)$$

$$V_{c_2} = V_{c/b} + V_b = V_d \quad (3.6)$$

From the equation (3.5), we get

$$V_b = V_{c/b} \quad (3.7)$$

From equation (3.6), upon substituting (3.7), we get

$$V_b + V_b = V_d ; \quad \therefore \quad 2V_b = V_d$$

and

$$V_b = \frac{V_d}{2} \quad (3.8)$$

Therefore, the velocity of the yoke is one-half that of the drive rack, which is the relationship desired for correct positioning of the mid plane source-detector. The same kinematic arrangement is applied to provide the quarter plane radiation source-detector positioning by mounting drive racks to the yoke positioning the mid plane source-detector (yoke 1). The quarter plane yoke (yoke 2) then is driven at half the mid plane velocity which is one-fourth the moving platen velocity, as desired. To attain the three-quarter plane yoke positioning, a compound gear train is required. Drive racks mounted to the quarter-plane positioning yoke rotate input gears. These mesh with gears secured to the output shafts in a 3:1 step-up ratio. This gives a multiplication of three to the angular velocities of the output shafts compared to the

input shafts. Output gears three times the diameter of the driven gears on the output shafts then convert the increased angular velocities to linear velocity of the three-quarter plane yoke (yoke 3) through engagement with racks mounted to the yoke.

The resulting mechanical device consists of three yokes and a system of gears and racks needed to drive them. The driven yokes are positioned across the top of the press and extend down both sides of the press, to the location position of the radiation source and detector. The yokes move on linear bearings relative to fixed precision rods mounted to a top plate which in turn is attached to the press upper platen. Rollers mounted to the vertical members of the yokes operate in guide channels fixed to the side plates of the base frame to restrain lateral movement of the yoke arms ( vertical members ).

To meet drive train requirements previously defined while applying symmetrical forces to vertical members of each yoke, two racks, one on each side of the press, attached to the moving platen drive gears which rotate on shafts that are fixed through bearing housings to the first yoke, one to each vertical member on opposite side of the press. These gears also mesh with identical stationary racks fixed to the upper platen of the press. Thus the first yoke moves at half the speed of the platen, keeping the radiation source and detector always at the center plane of the mat thickness. A second set of racks are attached to the first yoke which move gears with shafts fixed to the second yoke. The gears also mesh with identical stationary racks fixed to the upper platen of the press. The second yoke moves at half the speed of the first yoke. Racks connected to the second yoke drive systems

of gears which multiply the speed of the third yoke (Figures 3.3 and 3.4). The third yoke moves at three times the speed of the second yoke. With this rack and pinion arrangement of gears and yokes, the radiation sources and detectors remain at constant proportions of 50%, 25% and 75% of the press opening distance at all times during pressing.

The measurement of density is taken in fixed positions relative to X-Z coordinates of the mat; the radiation source and detector do not move relative to mat width or length.

The radiation sources and detectors are attached to the yokes via mounting brackets designed for maximum flexibility in position and adjustment. The radiation sources are placed in shop-made tubes with slits 1mm ( 0.0374 inch ) high and 12 mm ( 0.4724 inch ) wide in the end. These tubes are long enough to collimate the radiation source and thick and dense enough to serve as the radiation shielding for the sources. The detectors are mounted in holders with a 1mm ( 0.0394 inch ) high by 2mm ( 0.0787 inch ) wide collimating slits.

Temperatures of 177-204<sup>0</sup>C (350-400<sup>0</sup>F) are required for cure of most adhesive systems used in the manufacture of wood composite panel products. Therefore, an insulator pad is placed between the mechanism and press to allow the mechanism to perform satisfactorily under the temperatures required.

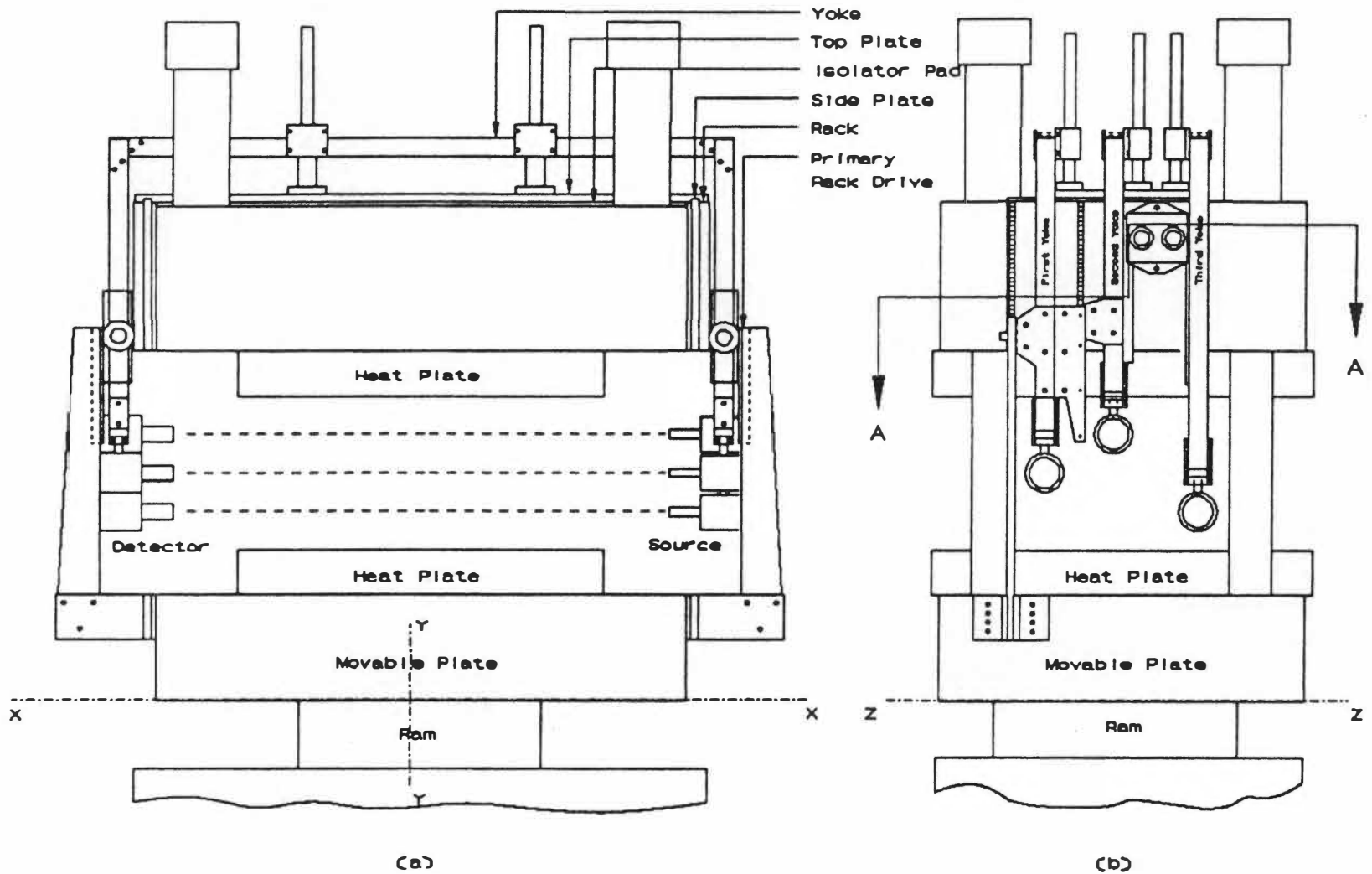


Figure 3.3 - Front View (a) and Side View (b) of yoke-translation device for translocation of sources and detectors in fixed horizontal planes relative to the mat height.

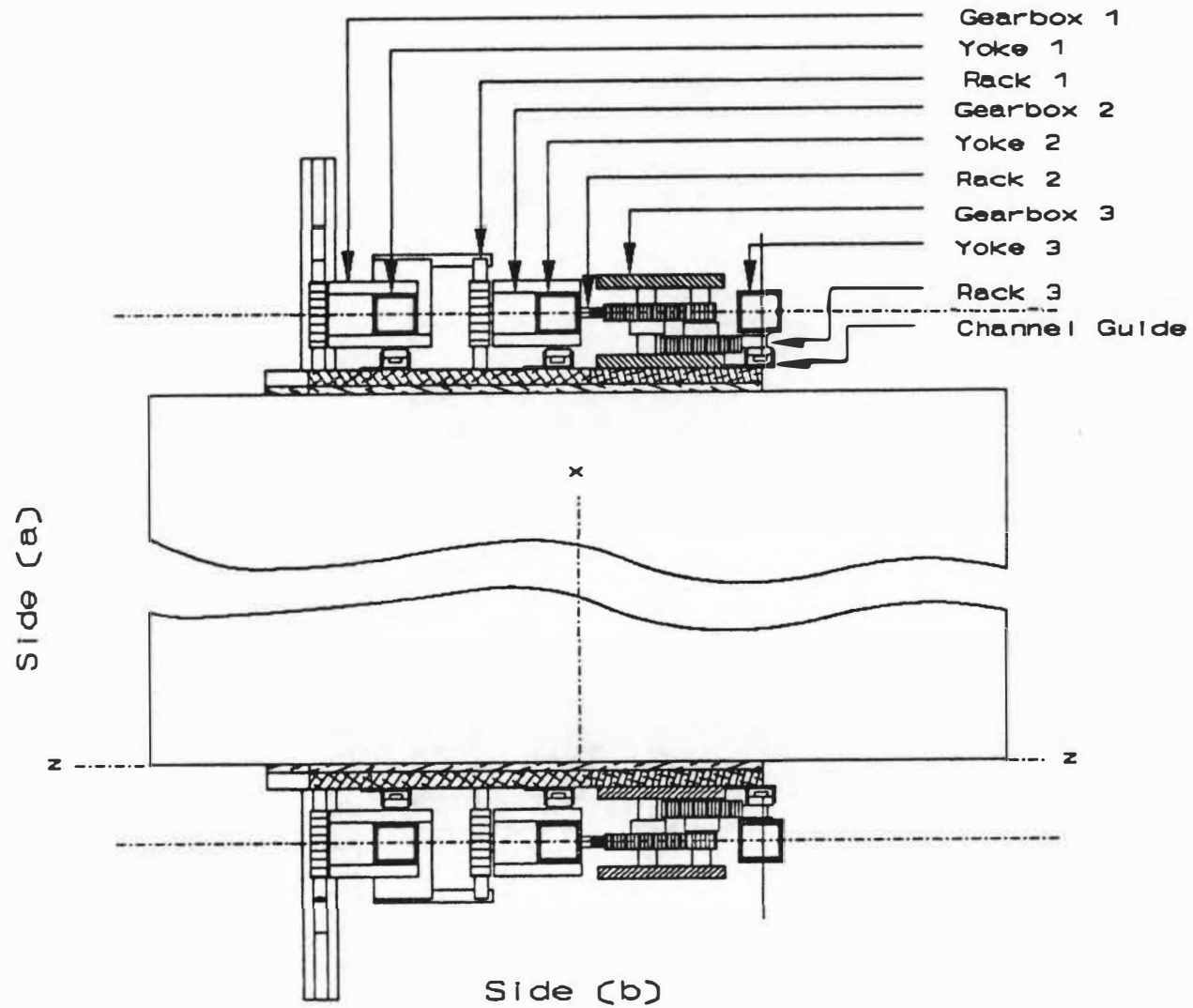


Figure 3.4 - Section A-A of the mechanical device.

## DEFINITION OF MAJOR COMPONENTS

The final mechanical device consists of racks and pinions ( small gears ) gearboxes, yokes, detectors and sources as defined in the previous section. Gears and yokes have been numbered in increasing order according to the positive direction of Z-axes on the Y-Z plane (Figure 3.5). All yoke and drive components are in duplicate, one on each side of the press. Gears engaging both fixed and moving ( drive ) racks are mounted on each side to both yoke 1 and yoke 2. Yoke 2 is driven by yoke 1 and yoke 3 is driven by yoke 2 through gearboxes mounted to each side of the press upper platen. Racks mounted to the lower platen of the press drive yoke 1. The Z-axes ( shaft longitudinal axes ) of the rack engaging pinions on yokes 1 and 2 are in the same Y-Z plane as the vertical axes of symmetry of the yoke arm tubes. The pinion shafts are mounted through bearings secured in housings attached to the yoke vertical arms to guarantee strength of the system ( gear and yoke ) and perfect, ninety degree angles between shaft centerlines and yoke faces. The yokes are square cross-section tubes that extend across the press in inverted "U" configuration. Sources and detectors can be perfectly aligned because they are attached to the yokes through adjustable connections.

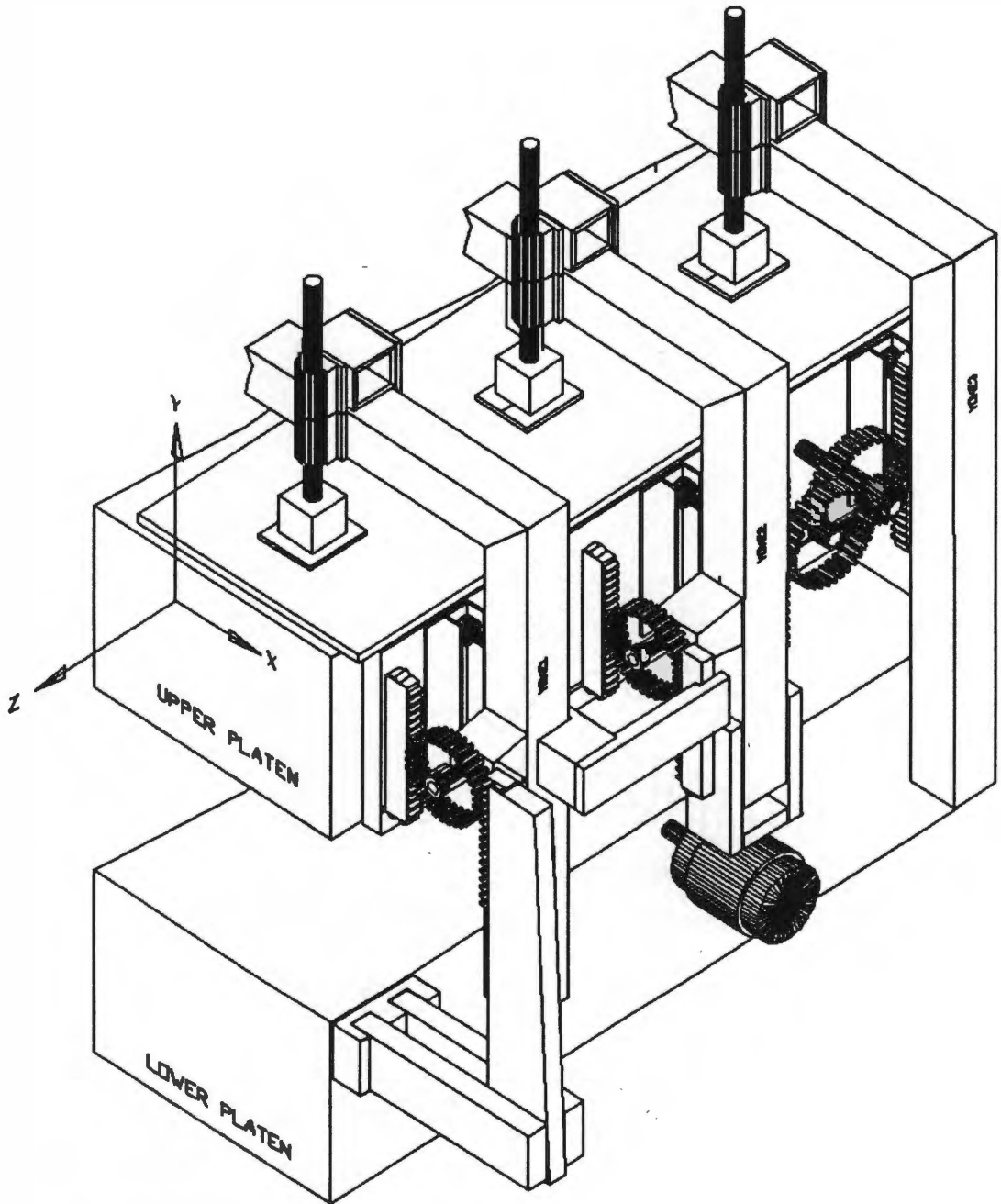


Figure 3.5 - Mechanical device on the press

## **CHAPTER 4**

### **COMPONENT DESIGN AND FABRICATION**

#### **BASE PLATE AND ASSOCIATED COMPONENTS**

All components to be fixed to the upper platen of the press are attached to an inverted "U"-shaped base plate which attaches to the upper platen after correct orientation is accomplished through alignment screws.

Placement of a base plate on the top and the sides of the press was necessary because of the uneven surfaces of the press. The accuracy needed for the kinematic mechanism required use of the base plate to correctly assemble the components. The top and sides of the base plate are made from 12.7 mm (0.5 inch) aluminum plate machined for flatness. An insulator pad was placed between the base plate and the press to reduce the heat transmission from the press to the plate and avoid risk of failure of the mechanical device as a result of thermal expansion of its components. The material to insulate the press from the mechanical device was a teflon pad with thickness of 6.35 mm (.25 inch). The decision for using a teflon pad was based on the area required for insulation, thermal properties, price, and the workability of the material.

Supports for the linear bearings and shafts placed on the top of the press were

designed to accommodate to shaft and linear bearing dimensions. The supports were made from aluminum and bolted to the top plate (figure 4.1).

The linear bearings are adjustable diameter pillow blocks with super ball bushing bearings and seals at both ends (Thompson model SPB-12-ADJ (Thompson, 1991)). Solid stainless steel 19.05 mm (.75 inch) nominal diameter shafts used in this project were hardened and ground to precise diameter dimensions of

19.0373/19.0246mm (.7495/.7490 inches ). Two linear bearings connected to each shaft react moments generated by forces in the X-Y and Y-Z planes.

The side plates were attached to the top plate in machined rectangular cross-section grooves to maintain 90 degree joints between top and side plates. The joint were secured with machined screws. Racks and gearboxes were attached to the side plates.

### SOURCE/DETECTOR ALIGNMENT

The alignment between detector and source are partially guaranteed by attaching both to the same yoke. In addition, the yoke vertical arms are restrained

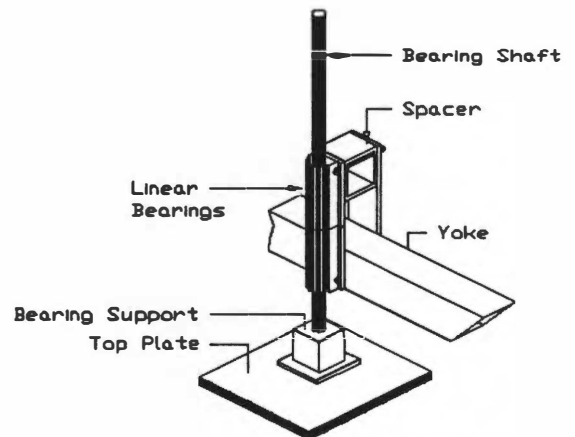


Figure 4.1 - View of the linear bearings positioning yoke at two positions symmetrically placed on top of press.

from lateral movement by guide bearings rolling in channel guides. However, some deviation was expected because of build up of fabrication tolerance. Consequently, adjustable attaching means were designed to allow alignment (Figure 4.2).

### YOKE-TRANSLATION COMPONENTS

The yoke translation components consist of sets of gears and racks placed in a way to keep the proportional movement of the yokes according to the requirement of the project as previously explained (Chapter 3). The characteristics of the chosen gears are as follow ( for yoke 1 and yoke 2 pinions):

Pitch diameter (  $d$  ) = 50.8mm (2 inch)

Number of teeth (  $N$  ) = 32

Face Width (  $W$  ) = 12.7mm (0.5 inch)

Bore diameter (  $Bd$  ) = 19.05mm (0.75 inch)

Pressure angle (  $\phi$  ) = 20 degrees

Material = 303 stainless steel

Diametral pitch (  $dp$  ) =  $N/d = 16$

Velocity of the pitch line (  $Vp$  ) =  $(\Pi * d * n)/12$

Revolutions per minute (  $n$  ) is a function of the maximum velocity of the press closing which is 19.05mm/sec (0.75 inch/sec). Therefore,  $n$  is equal to 7.16 rpm.

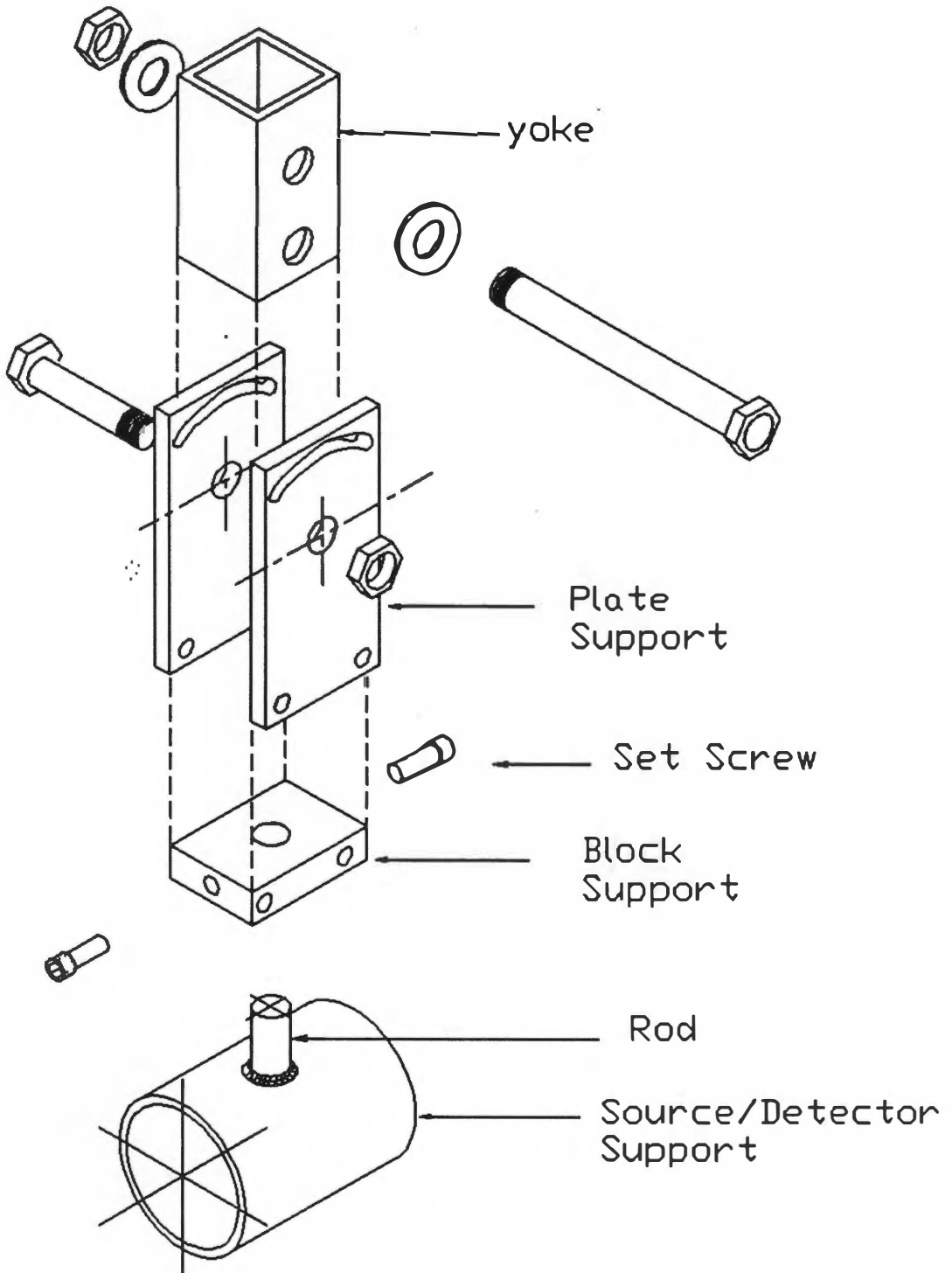


Figure 4.2 - View of the detector/source attachment assembly.

## SPEED MULTIPLIER MECHANISM

The project requires that the third yoke have three times the speed of the second yoke in order to maintain the radiation source and detector at required proportion of the press opening distance during the pressing time (Figure 4.3). The speed multiplier mechanism is a compound gear train consisting of 3 gears and two shafts. The rack attached to yoke 2 (Ry2) meshes with the gear 1 (G1), while G1 meshes with the pinion (P) to increase the rotational speed 3 times. Gear 2 is fixed to the same shaft as the pinion. With this arrangement, the rotational motion of the pinion shaft is converted to linear motion by gear 2 (G2) driving rack 3 (Ry3). This gear-rack train drives rack 3 to travel three times the velocity of rack 2.

The large gears of the speed multiplier mechanism have the following specifications (Table 4.1):

Table 4.1: Characteristics of speed multiplier gears

Pitch diameter d (inches)	Number of teeth N	Bore b (inches)	Pressure angle $\phi$ (degrees)	Diametral Pitch dp (N/d)
2.25	36	0.5	20	16
Material		303 Stainless Steel		

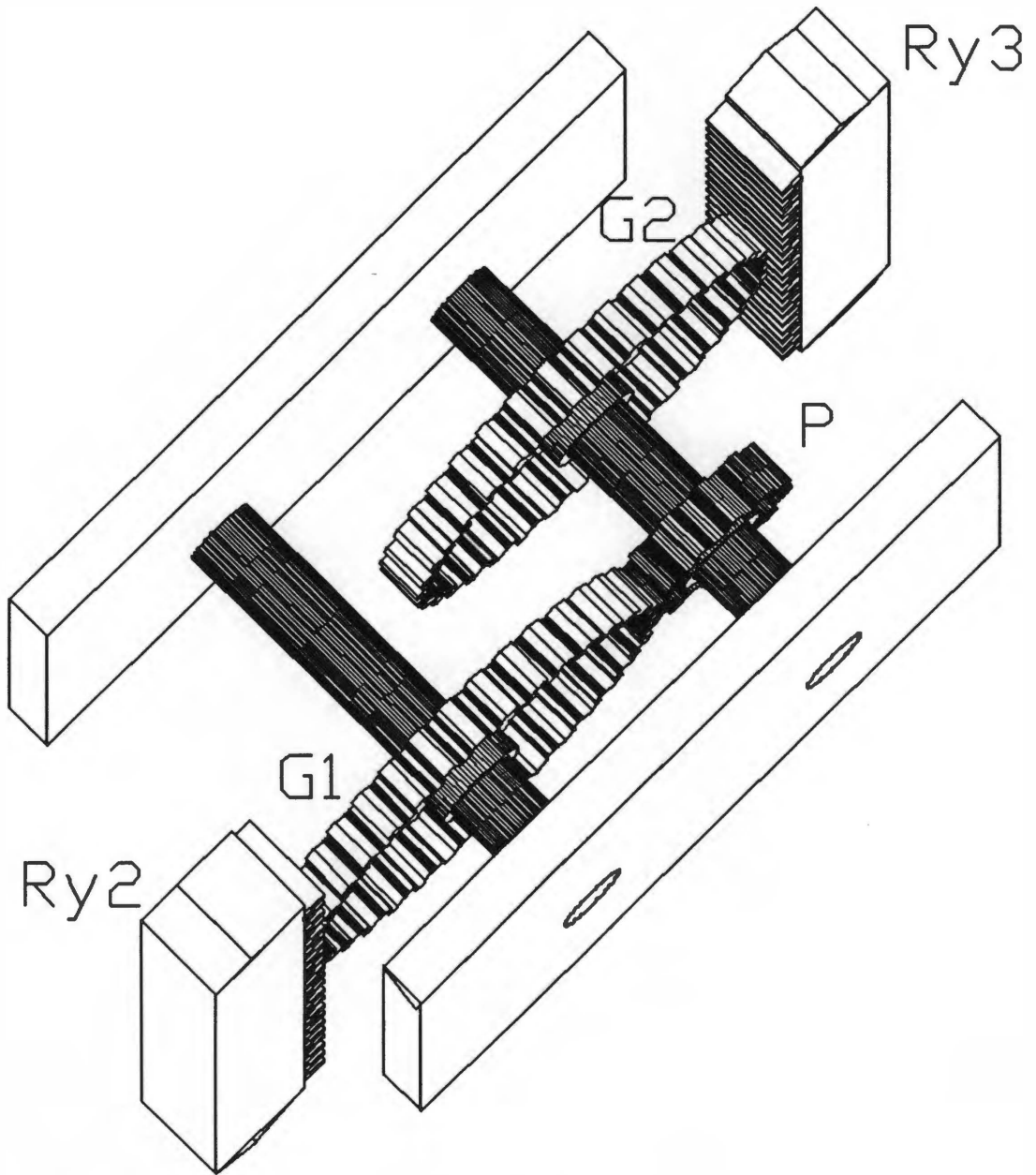


Figure 4.3 - Pictorial view of the speed multiplier mechanism.

The mechanism requires that the angular velocity of the pinon ( $\omega_p$ ) be three times the angular velocity of the gear ( $\omega_g$ ) (Figure 4.4). Therefore, the pitch

diameter of the pinion (  $d_p$  ) can be determined by using the fundamental law of gearing and velocity (Deutschman, 1975).

$$\frac{\omega_g}{\omega_p} = \frac{N_p}{N_g} = \frac{d_g}{d_p} = \frac{1}{3} \quad (4.1)$$

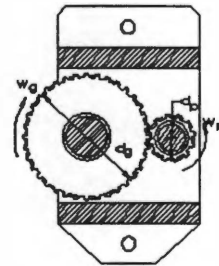


Figure 4.4 - View of the gears of the speed multiplier mechanism.

Therefore, the pinion has a pitch diameter of 19.05mm (0.75 inch) and the number of teeth is 12. In addition, the value of the standard center distance (  $c$  ) is 38.1 mm (1.5 inches). The number of teeth in contact is determined by the following equation (Deutschman, 1975).

$$cr = cr_g + cr_p \quad (4.2)$$

where  $cr_g$  and  $cr_p$  are the contact ratio of the gear and pinion respectively and these quantities are given by the following equation.

$$cr_i = \frac{\sqrt{(r_i + a_i)^2 - r_i^2 \times \cos^2 \phi} - r_i \times \sin \phi}{pc \times \cos \phi} \quad (4.3)$$

where  $i$  can be either gear (g) or pinion (p),  $a$  is the value of the addendum,  $pc$  is the circular pitch, and  $\phi$  is the pressure angle. Substituting the values of the above variables into the equation 4.3, the number of teeth in contact between the gear and pinion is 1.56. The normal acceptable range is from 1.2 to 1.6 with the greater value preferred.

The existence of interference is determined by comparing the value of the maximum possible addendum radius without interference, calculated by equation 4.4 following, with the actual addendum radius of the gear concerned (Juvinal 1983).

$$r_{a(\max)} = \sqrt{r_b^2 + c^2 \times \sin^2 \phi} \quad (4.4)$$

where  $r_{a(\max)}$  is the radius of maximum allowable addendum circle without interference  $r_b$  is the base circle radius,  $c$  is the center distance of the two gears in mesh, and  $\phi$  is the pressure angle of the gear system. The variable  $r_b$  is equal to the pitch radius ( $r_p$ ) times the cosine of the pressure angle. Substituting in equation 4.4 for the pinion (the member most likely to have interference) gives the value of  $r_{a(\max)}$  equal to 0.662. The actual value for radius of the addendum circle for the pinion is 0.4375 from:

$$R = r_p + a \quad (4.5)$$

Therefore, inference will not occur because the actual radius of the addendum circle is less than the maximum allowable radius.

## GEAR HOUSING

The step-up gear housing was designed according to bearing manufacturer's recommendations (Torrington Brg Co., 1988). The criteria used were for very low runout and high radial rigidity which require an average line-to-line fit between bearing bore and shaft diameter and average bearing outside diameter to housing

bore fit of 0.0000 mm tight to 0.0008mm ( 0.0003 inch) loose. Shaft and housing shoulders, along with spacers, were used to limit end play to that needed for thermal expansion. Figure 4.5 shows an exploded view of the assembly which used standard precision ball bearings.

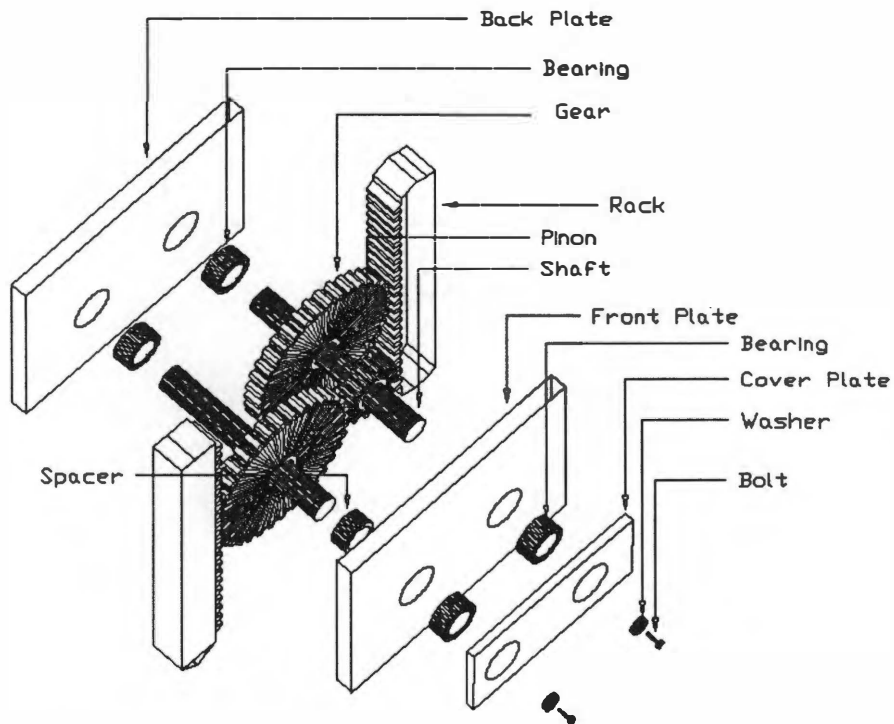


Figure 4.5 - Step-up gear, housing, shaft assembly.

Gearboxes 1 and 2 were designed to attach the gears operating between fixed and moving racks to yoke 1 and yoke 2, respectively, and to provide for precision pitch line fit-up between gears and racks. These housings were also designed to give strength and rigidity to the gear and yoke system. Lateral plate assemblies positioned these gears boxes correctly with respect to the yokes. Figure 4.6 shows gear box 1 and attaching components. Figure 4.7 shows gear box 2 and attaching components.

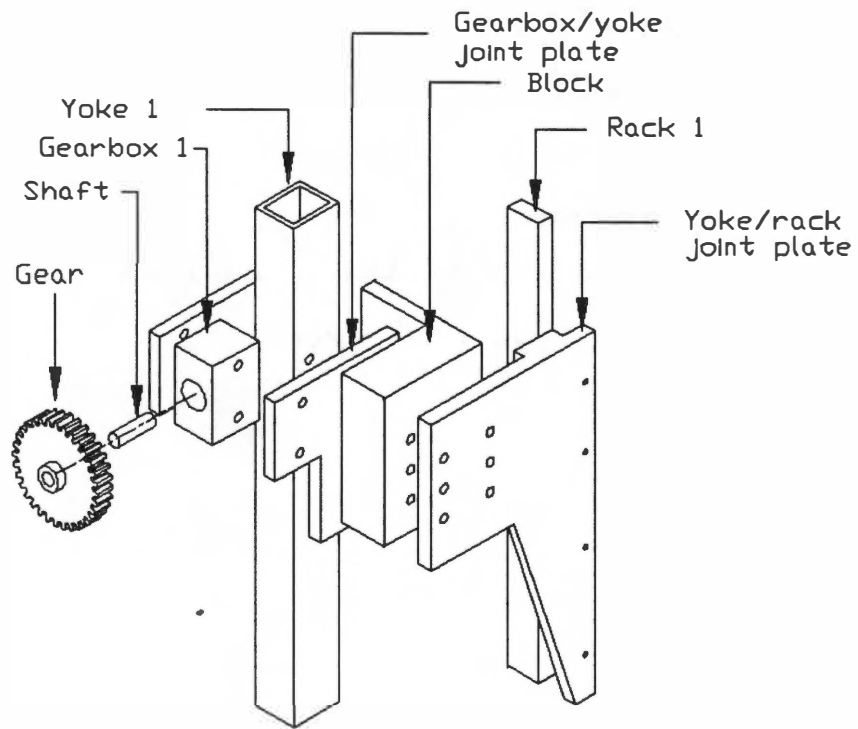


Figure 4.6 - Attachment of gear box 1 to yoke and rack.

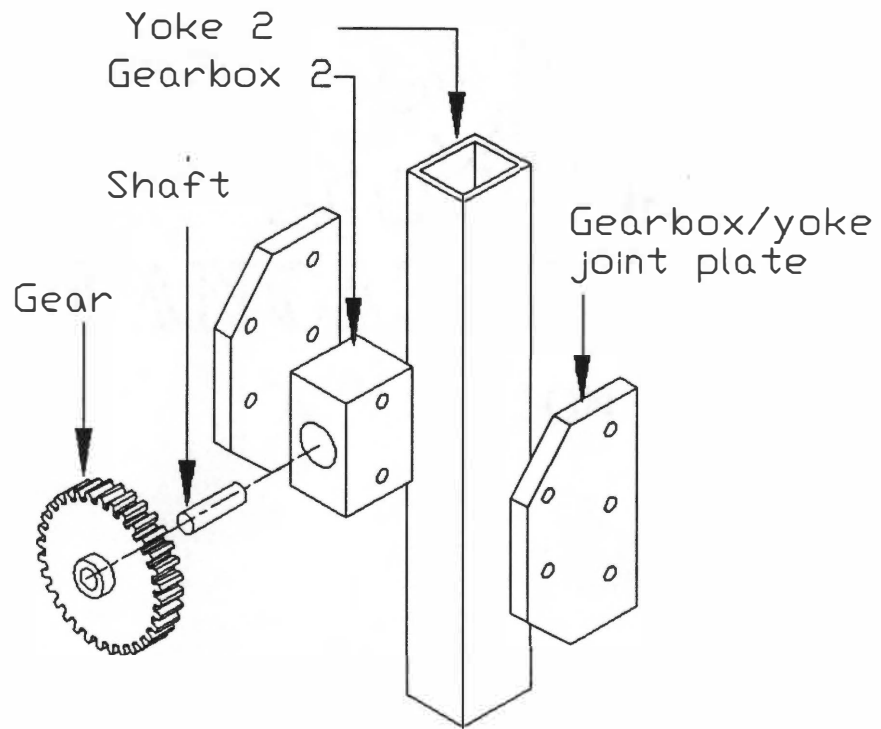


Figure 4.7 - Attachment of gear box 2 to yoke.

## PLATEN DRIVE RACK COMPONENTS

The platen drive rack assemblies are important components in the mechanical device because they drive yoke 1 which drives the other two yokes. These components required special attention to strength and deformation because any excess deformation of the support for the primary drive would jeopardize the precision of the system. The support structure for the primary drive is the component which transmits the movement of the press to the entire drive train; it must resist the overall load. A beam with variable cross section was designed as the primary drive support to give maximum rigidity to the system ( figure 4.8 ). Four alignment screws were included in each mounting plate to allow precise alignment of the drive rack pitch line with that of the fixed rack fastened to the side plate on the upper platen of the press.

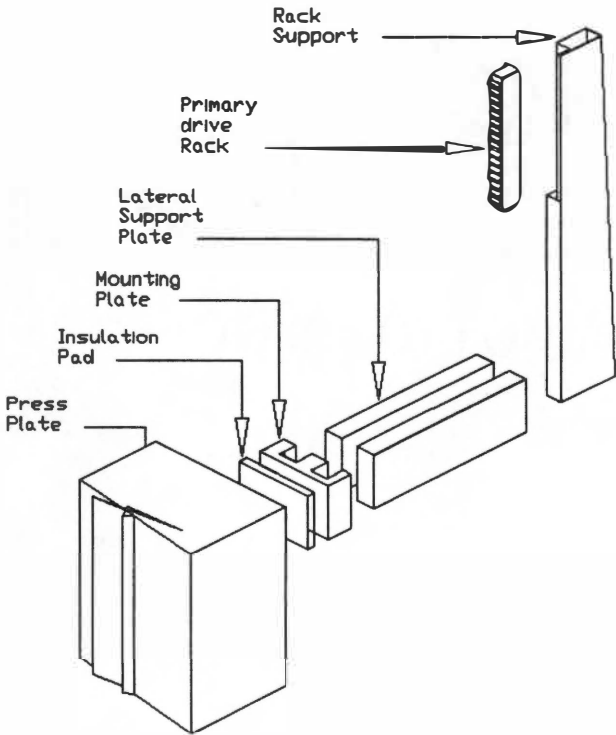


Figure 4. 8 - Primary drive components (right side shown, left side opposite).

## **CHAPTER 5**

### **EVALUATION TESTS**

The experimental procedure for testing the mechanical device consisted of installation, calibration, and measurement of the accuracy and backlash of the mechanical device, and of measuring the mat density during the pressing cycle.

#### **INSTALLATION OF THE DEVICE**

The first step in assembly of the mechanical device on the press was to place the top and side plate assembly on the press upper platen, align it to the press reference surface, then secure it in place with capscrews. The alignment of the top plate was done with four alignment screws. A precision level was used to insure the top plate upper surface was parallel to the upper surface of the press lower platen heated plate. The product contacting surface of the upper and lower heat plates had been machined previously to be parallel within 0.08 mm ( 0.003 inch ). The correct angles between the top plate and the side plates were achieved by using the four alignment screws on each side plate.

The second step was to attach the drive rack supports to the movable platen of the press. A width gage with a dimension equal to the sum of the pitch dimensions of the racks and gear was utilized during the assembly to guarantee the distance of

the driven rack support related to the side plate. The alignment of the drive rack with the side plate was determined with the help of dial indicators with precision of 0.0125 mm (0.0005 inch). The drive rack supports were adjusted by using the alignment bolts on the mounting plate to bring the drive rack pitch line parallel to the fixed rack pitch line within 0.051mm (0.002 inch).

The third step was to assemble the yoke and gears boxes to the upper plate assembly which had been previously aligned and fastened to the press upper platen. Yoke 3 was the first assembled on its guide rods. After yoke 3 had been placed on the press, the channel guide situated behind this yoke was adjusted to keep the guide rollers fastened to the yoke in contact with the inside surface of the guide channel. After yoke 2 had been assembled on its guide rods, gear boxes 3 were assembled on the side plates fastened to the upper platen of the press. Gear boxes 2 were attached to yoke 2 in position to be in alignment with the driving and fixed racks engaging the pinions. The guide rollers fastened to yoke 2 located behind gear box 2, were fit in the guide channels and the channels adjusted to have the inside front surfaces of the guide channel in contact with the guide rollers. Yoke 1 was the last to be assembled on its guide rods. The drive racks engaging its pinions had to be adjusted vertically on the drive rack support beams for a perfect engagement between the teeth of the pinions and the driving and fixed racks engaging them. The holes on the drive rack supports were slotted to allow this final adjustment of the drive racks and gears. The guide rollers attached to yoke 1, located behind gear boxes 1, were brought into contact with the front inside surfaces of the guide channels engaging the rollers by

lateral adjustment of the guide channels fastened to the side plates on the press upper platen.

### **CALIBRATION OF SOURCE AND DETECTOR HOLDING TUBES INITIAL VERTICAL POSITION**

The source and detector supports were designed to allow adjustment of the distance from the center of the source/detector holding tube to the reference surface (lower surface of heated plate of upper platen). Since it is more convenient to measure distance from the top surface of the heated plate of the lower platen of the press, this was the surface used as the reference to set initial position of the source/detector tube centers for calibration. An internal micrometer was used to determine the exact distance between top and bottom press plate inside surfaces with the press in the maximum open position. The average of the nine measurements (three at evenly spaced intervals under each yoke centerline across the width of the press heated platen) was 240.0584 mm (10.0023 inches). This was the true value maximum opening distance (X) used for setting source and detector initial centerline position above the top surface of the heated plate of the press lower platen.

The initial positions required to sense half plane, quarter plane and three quarter plane densities of the mat being pressed were half, quarter and three quarters, respectively, of the maximum press opening of 240.0584mm (10.023 inches).

Three gage blocks, a precision ground rod of 19.05mm (0.7500 inches) diameter, and two plugs (for precise fit in source and detector holding tubes) were fabricated and used with a precision v-block to calibrate initial position of the source and detector holding tubes attached to each yoke. The heights of the gage blocks were determined by the difference between the height required for the centerline of holding tubes for each yoke and the fixed distance from the center of the precision ground 19.05 mm (0.7500 inch ) rod clamped in the precision v-block and the lower surface of the v-block. The plugs had outside diameter equal to the inside diameters of the source and detector tubes, respectively, and both plugs had inside diameter reamed to be exactly equal to the diameter of the precision rod. Both gage blocks and plugs were constructed with a precision of  $\pm 0.0127\text{mm}$  (0.0005 inch).

The calibration procedure involved the following steps: For yoke 1, after the source and detector attaching assemblies had clamp screws loosened to allow adjustment, the plugs were set in the source and detector support tubes. The gage block was placed on the lower platen heat plate upper surface midway between the source and detector tube midpoints. The v-block clamped to the precision ground rod was set over the gage block and the precision ground rod was inserted in the source and detector plug bores, adjusting the tube attaching assemblies to allow this. Once aligned to the precision ground rod and plug reference planes, the attaching assemblies were tightened to hold position, and the plug and rod were removed. In this way, the correct initial height for the center of the source and detector holding tubes for yoke 1 was achieved. The same procedure of calibration was followed to

attain the proper setting for the initial centerline positions for source and detector holding tubes attached to yoke 2 and yoke 3.

### **MEASUREMENT OF THE ACCURACY AND BACKLASH**

Three tests were made for measuring the accuracy and backlash of the mechanical device. The first test was to determine the accuracy of the instruments used, the second test to determine the tracking accuracy of the source and detector centerlines on an individual yoke and the third test was to determine the backlash build-up in the rack-gear drive train between yoke 1 and yoke 3.

Two direct current linear variable differential transformers ( LVDT's ) connected to a personal computer were used in these tests.

#### **Accuracy of the instrument**

The accuracy of the instruments used was determined to understand the magnitude of error of the device. Two LVDT's were fixed to the press upper platen by magnetic base and attaching assemblies. The core rods of the LVDT's were positioned in contact with the upper centerline of the outside surface of a single source holding tube. The movement of the single source holding tube during the press cycle was followed by both LVTD cores and output position data recorded. A linear regression analysis then was made between data obtained from the two LVDT's. Figure 5.1 show a displacement and time graph from data take during a

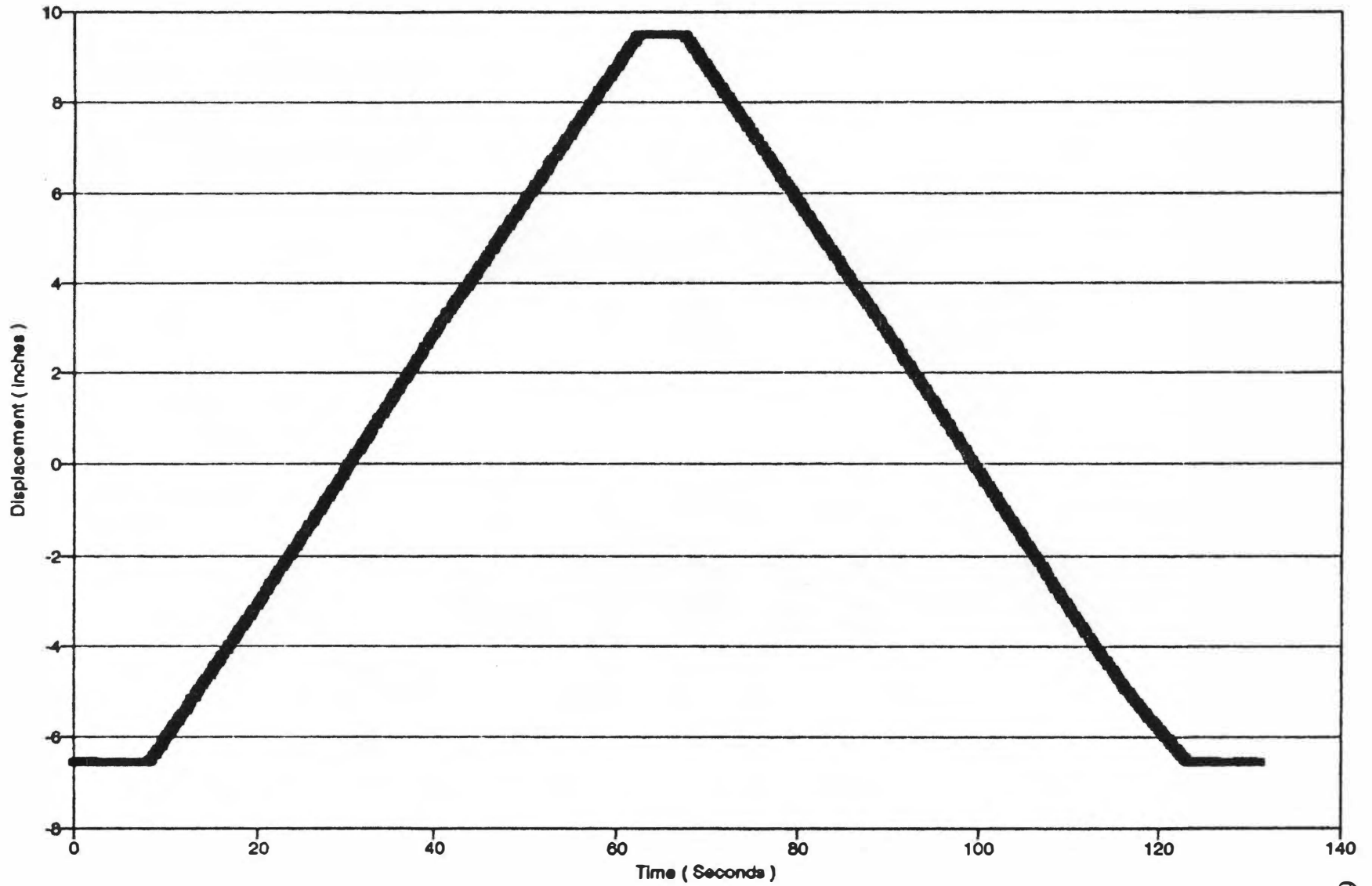


Figure 5.1 - Yoke displacement during press time.

typical press cycle of these tests. The bottom horizontal line marks the begin and end positions of the sensed line at the top of the source holding tube when the tube is in the "home" position. The left inclined line is displacement versus time with the press closing. The top horizontal line is the upper position during dwell of the press at the closed position. And the inclined right line is displacement versus time with press opening and returning to "home" position.

The relationship between the data obtained from both LVDT's was determined through regression analysis. The variables L0 and L1 refer to the data obtained from the LVDT's hooked to channel 0 and channel 1, respectively, of the computer. The objective of using the regression analysis was to determine the ratio between the displacement detected by L0 and L1 since the expected ratio is 1. With core rods of both LVDT's being positioned at the same plane, the displacement of both LVDT's should be equal; otherwise, the instruments or method of test is inaccurate. Five sets of data were taken and analysed. In addition, estimated means for values based on displacements of 1, 2, 3, 4 and 5 inches for L1 were calculated for L0 based on the equation obtained from the regression analysis. Table 5.1 shows a summary of the regression analyses from this series of tests.

According to the  $R^2$  values obtained (Table 5.1), 99.99% of the variation of L0 is explained by the variation of L1 for the models studied. The estimates calculated showed that the standard error of estimate increases when L1 increases. Table 5.2 show the average of the estimate means for the five regression analyses

Table 5.1 - Summary of regression analysis from data obtained in the first series of tests.

Reg	Equation	L1	L0	Std.Er.Est.
1	$L0 = -.0004 + 0.998677L1$ $R^2 = 0.99991$	1	0.99828624	0.00022748
		2	1.99696357	0.00018491
		3	2.99564089	0.00021093
		4	3.99431822	0.00028750
		5	4.99299554	0.00038559
2	$L0 = 0.004001 + 0.99869L1$ $R^2 = 0.9999$	1	1.00269613	0.00022098
		2	2.00139039	0.00018021
		3	3.00008465	0.00020762
		4	3.99877891	0.00028413
		5	4.99747317	0.00038123
3	$L0 = -.01084 + 0.997518L1$ $R^2 = 0.99998$	1	0.98667763	0.00037036
		2	1.98419636	0.00028884
		3	2.98171509	0.00027938
		4	3.97923382	0.00034790
		5	4.97675256	0.00046085
4	$L0 = 0.00139 + 0.998642L1$ $R^2 = 0.99990$	1	1.00003900	0.00020817
		2	1.99868178	0.00017441
		3	2.99732457	0.00020842
		4	3.99596735	0.00028705
		5	4.99461013	0.00038379
5	$L0 = 0.00043 + 0.999435L1$ $R^2 = 0.99943$	1	0.99986832	0.00035417
		2	1.99930429	0.00028801
		3	2.99874026	0.00034472
		4	3.99817623	0.00048280
		5	4.99761220	0.00065248

Table 5.2 - Average of deviation measured between L1 and estimate (first series).

L1 (inch)	Estimate (L0) (inch)	L1-Estimate (inch)	Average Deviation (inch)
1	0.997584	0.002416	0.005285
2	1.996107	0.003893	
3	2.994701	0.005299	
4	3.993259	0.006705	
5	4.991889	0.008111	
Reg	Interval Estimation L1 = 5 inches		Largest Deviation
1	4.992002 , 4.993989		0.006011
2	4.996491 , 4.998455		0.001545
3	4.975565 , 4.977940		0.022060
4	4.993622 , 4.995599		0.004401
5	4.995931 , 4.999293		0.000707
Average			0.006945

and their predicted interval. From table 5.2, it can be concluded that the average deviation (L1-estimate) is 0.005285 inches and the average of the difference between the largest deviation and L1 among the five points considered is 0.006945 inches.

### **Tracking accuracy of the source and detector**

The second series of tests consisted in the determination of the accuracy of the source and detector coincident movement of the same yoke. The LVDT's were used on the same yoke but one was placed for measuring the displacement of the source support (L1) and the other the displacement of the detector support (L0). The statistical procedure used in the previous test series was repeated in this series of tests. Table 5.3 shows a summary of the analyses for this series of tests. Table 5.4 show the average of estimated means and its predicted interval assuming that the equation determined for this series of tests adequately fits the data. According to table 5.4, the average of the deviation among the regressions considered with five data points used for each regression is 0.007942 inch; in addition, the average of the largest error is 0.013545 inch. If we assume that we can subtract the deviation of the previous series of tests from deviation of this test series, it is possible to say that this difference is the accuracy of the device. Therefore:

$$\text{Deviation (average)} = 0.007947 - 0.005285 = 0.002662 \text{ inches.}$$

$$\text{Deviation (largest)} = 0.013545 - 0.006945 = 0.0066 \text{ inches.}$$

Table 5.3 - Summary of regression analysis from data obtained in the second series of tests.

Reg	Equation	L1	L0	Std.Er.Est.
1	$L0 = 0.0004 + 0.997541L1$ $R^2 = 0.99985$	1	0.99795817	0.0002948
		2	1.99550010	0.00023773
		3	2.99304203	0.00028088
		4	3.99058395	0.00038110
		5	4.98812588	0.00050551
2	$L0 = -0.00256 + 0.99819L1$ $R^2 = 0.9998$	1	0.99563203	0.00034430
		2	1.99383187	0.00026809
		3	2.99203170	0.00029002
		4	3.99023153	0.00039403
		5	4.98843136	0.00053415
3	$L0 = -0.00538 + 0.99847L1$ $R^2 = 0.99998$	1	0.99293850	0.00036090
		2	1.99141573	0.00027662
		3	2.98989297	0.00029682
		4	3.98837020	0.00040620
		5	4.98684743	0.00055427
4	$L0 = 0.00681 + 0.998031L1$ $R^2 = 0.99998$	1	0.99871384	0.00035617
		2	1.99674629	0.00027906
		3	2.99477868	0.00029258
		4	3.99281107	0.00038736
		5	4.99084347	0.00052076
5	$L0 = 0.00224 + 0.99611L1$ $R^2 = 0.99984$	1	0.99872647	0.00029294
		2	1.99523819	0.00024023
		3	2.99174992	0.00027664
		4	3.98826164	0.00037719
		5	4.98477336	0.00050492

Table 5.4 - Average of deviation measured between L1 and estimate (second series).

L1 (inch)	Estimate (L0) (inch)	L1-Estimate (inch)	Average Deviation (inch)
1	0.996794	0.003206	0.007947
2	1.994447	0.005553	
3	2.992299	0.007701	
4	3.988923	0.011077	
5	4.987804	0.012196	
Reg	Interval Estimation L1 = 5 inches		Largest Deviation
p1	4.986824 , 4.989428		0.013176
2	4.987055 , 4.989807		0.012945
3	4.985420 , 4.988275		0.014580
4	4.989502 , 4.992185		0.010498
5	4.983473 , 4.986074		0.016527
Average			0.013545

In other words, the average tracking accuracy of source and detector on a single yoke is within 0.003 inch assuming an instrument deviation of 0.005 inches. The maximum tracking deviation is 0.007 inches assuming an instrument maximum deviation of 0.007 inches.

### **Backlash of the drive train between yokes**

The third series of experiments was to determine the backlash in the drive train between yokes 1 and 3. One LVDT was placed on the source support of yoke 1 and the other on the source support of yoke 3. Readouts from the LVDT's were plotted as displacement versus time for a press cycle. Figure 5.2 shows the displacements of yoke 1 and yoke 3 during press closing time. Linear regressions between displacement and time for the two sources during press closing portion of the cycle were performed. The resulting equations are:

$$\text{For yoke 1: } Y_1 = a_1 + b_1 X;$$

$$\text{For yoke 3: } Y_3 = a_3 + b_3 X.$$

The parameters  $b_1$  and  $b_3$  are the velocities of the source supports of yoke 1 and 3 respectively. Therefore, division of  $b_3$  by  $b_1$  gives velocity ratio between yoke 3 and yoke 1 (Results are shown in table 5.4).

Table 5.5 shows a summary of the linear regression equations obtained from the data of the third test series and table 5.6 shows yoke 3 to yoke 1 velocity ratio and the difference between the initial yoke movement.

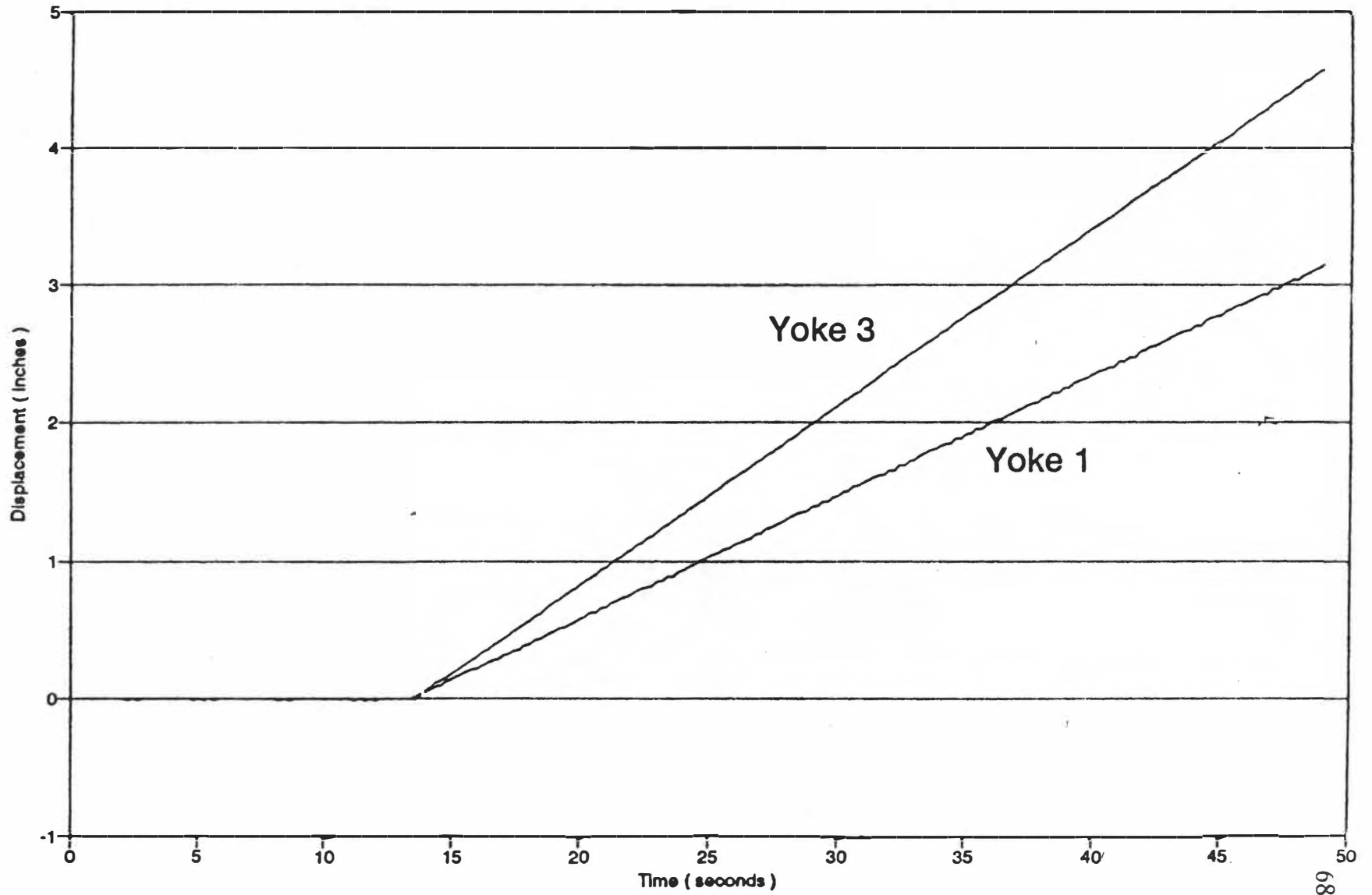


Figure 5.2 - Displacement yoke 1 and yoke 3 (press closing portion).

Table 5.5 - Summary of the regression analysis from data obtained in the third series of tests.

Test		Equation	R <sup>2</sup>	SEY <sub>est.</sub>
1	Yk 1	$Y = -0.45512 + 0.087676 X$	0.99	0.005511
	Yk 3	$Y = -0.81311 + 0.129699 X$	0.99	0.003232
2	Yk 1	$Y = -0.75623 + 0.087817 X$	0.99	0.000056
	Yk 3	$Y = -1.24523 + 0.129556 X$	0.99	0.000026
3	Yk 1	$Y = -1.17827 + 0.088148 X$	0.99	0.007506
	Yk 3	$Y = -1.75421 + 0.129258 X$	0.99	0.011889
4	Yk 1	$Y = -1.15654 + 0.089265 X$	0.99	0.011008
	Yk 3	$Y = -1.80771 + 0.129592 X$	0.99	0.004015
5	Yk 1	$Y = -0.97105 + 0.087570 X$	0.99	0.01472
	Yk 3	$Y = -1.4343 + 0.128951 X$	0.99	0.020394
6	Yk 1	$Y = -0.76669 + 0.088099 X$	0.99	0.005614
	Yk 3	$Y = -1.25932 + 0.129788 X$	0.99	0.003171

Yk 1 = Yoke 1; Yk 3 = Yoke 3.

**Table 5.6 - Relationship between velocities of yoke 3 and yoke 1.**

Test	Yoke 3	Yoke 1	Speed ratio
	b3	b1	Yoke 3/ Yoke 1
1	0.129699	0.087676	1.479298
2	0.129556	0.087817	1.475295
3	0.129258	0.088149	1.466374
4	0.129529	0.089265	1.451061
5	0.128951	0.087570	1.472547
6	0.129788	0.088099	1.473206
Velocity ratio average			1.469630

Since the expected velocity ratio between yoke 3 and yoke 1 is 1.5 and the mean detected ratio was 1.4696 (Table 5.6) the backlash of the drive train between the yokes is small enough to give a drive ratio accuracy of 97.97%. Therefore, the average of experimental data shows the accuracy of the position of yoke 3 relative to yoke 1 was within 98% of theoretically correct value. The inaccuracy involves the inertia of the system in addition to the inaccuracy of the measurement instruments and the variation in the press driven system.

## **EVALUATION OF DENSITY MEASUREMENTS DURING PRESSING**

### **Theoretical development and assumptions**

Following validation of the performance of the yoke-translation device on the press, density measurements were made while pressing laboratory panels to demonstrate correct application of principle and performance of the device.

The concept that attenuated radiation decreases exponentially with increasing board width ( $t$ ) coincides with known relationships for radiation methods used to measure density and moisture content.

Because the linear attenuation coefficient is constant, the logarithm ratio between emitted ( $I$ ) and attenuated radiation ( $I_0$ ) decreases linearly with increasing board width ( $t$ ). It was imperative for the first evaluation of this methodology that a linear relationship exist between  $t$  and  $\ln(I/I_0)$ .

Two assumptions were made during experimentation and data collection:

1. The edge of the board remains flat and perpendicular to the radiation source during pressing; i.e., spalting of the mat is at a minimum since the mat was prepressed and trimmed before placement in the press.
2. The horizontal density variation of the mat is minimal; normal forming methods for the mat should not introduce significant density variation within the horizontal planes being monitored during pressing.

### **System Description**

The yoke-translation device was mounted on the 24" by 24" 100-ton hydraulic hot press located at the Mengel Forest Products Laboratory, University of Tennessee, Knoxville. The hydraulic press is computer controlled for all press cycle parameters and is described by McFarland and Winistorfer (1991).

The radiation source ( $\text{Am}^{241}$ ), detector, and system electronics from the existing scanning gamma densitometry system were adopted for use on the press. The source and detector were mounted at the midplane sensing position of the device (yoke 1). The midplane source/detector holder maintains a relative position at 50 percent of mat thickness at all times during pressing. The radiation/detector system and peripheral equipment are described in several references (Moschler and Winistorfer, 1990; Moschler and Dougal, 1988; Winistorfer et al., 1986). Figure 5.3

is a schematic representation of the apparatus in-place on the press. The detector slit opening was adjusted to 1 mm in width by 10 mm in length for initial measurements.

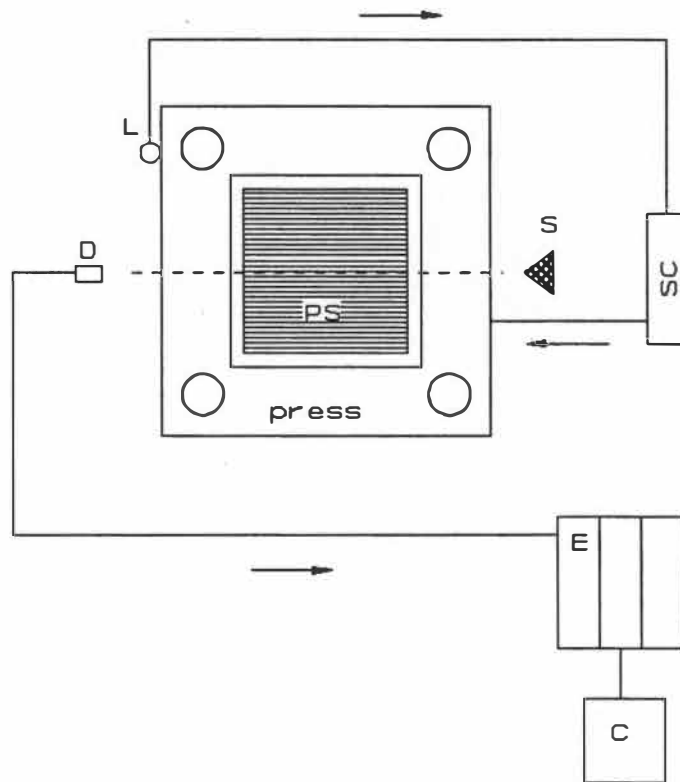


Figure 5.3 - Schematic representation of the gamma densitometer apparatus. SC) press digital servo controller; PS) sample; L) LVDT; S) source; D) photoscintillation detector; E) electronics for gamma detection; C) PC microcomputer.

### Calibration

Although system calibration has been described by Moschler and Dougal (1988) for the conventional laboratory arrangement of this scanning gamma densitometry system, an initial calibration was conducted for the  $\text{Am}^{241}$  source as

situated on the yoke-translation device.

Following the calibration procedure of Moschler and Dougal (1988), four rectangular sample blocks of red oak (*Quercus rubra*) were carefully machined to dimensions of 0.5 inch thickness, 10 inches in length, and widths (attenuation distance) of 2, 4, 6, and 8 inches, respectively. Linear measurements were made for each block, as were individual sample weights. Average moisture content of the blocks was 8.0%. Density of each block was calculated and is shown in Table 5.7

Thirty-second counts were taken at a single location on the radial surface of each block. The average of these counts was used to calculate the linear attenuation coefficient (Table 5.7). Figure 5.4 shows the relationship between the logarithm of count rate over air count and width. The average mass attenuation coefficient obtained from this calibration procedure was  $0.21 \text{ cm}^2/\text{g}$ . This value is in agreement with other reported wood mass attenuation coefficients as reviewed by Moschler and Dougal (1988).

### **In-situ measurements**

Laboratory mats were prepared for initial density measurements during pressing. Commercial Southern pine furnish and liquid phenol formaldehyde resin were used to fabricate 0.5 inch,  $42 \text{ lb}/\text{ft}^3$  lab panels. Furnish was blended in a cascading-action laboratory blender, with 4.5 percent resin solids based on oven-dry weight of the furnish. Mats were formed in a 16" by 16" forming box with a removable plywood bottom. After forming, a plywood top was used to prepress the

**Table 5.7 - Linear attenuation and mass attenuation of the calibrated sample.**

Sample	I	t	sp.gr.	$\mu_1$	$\mu_m$
Oak 2	174.1	5.1	0.76	0.1578	0.208
Oak 4	72.7	10.1	0.78	0.1662	0.213
Oak 6	34.6	15.24	0.75	0.1593	0.212
Oak 8	17.4	20.30	0.75	0.25314	0.204

sp. gr: Gravimetric determination of specific gravity.

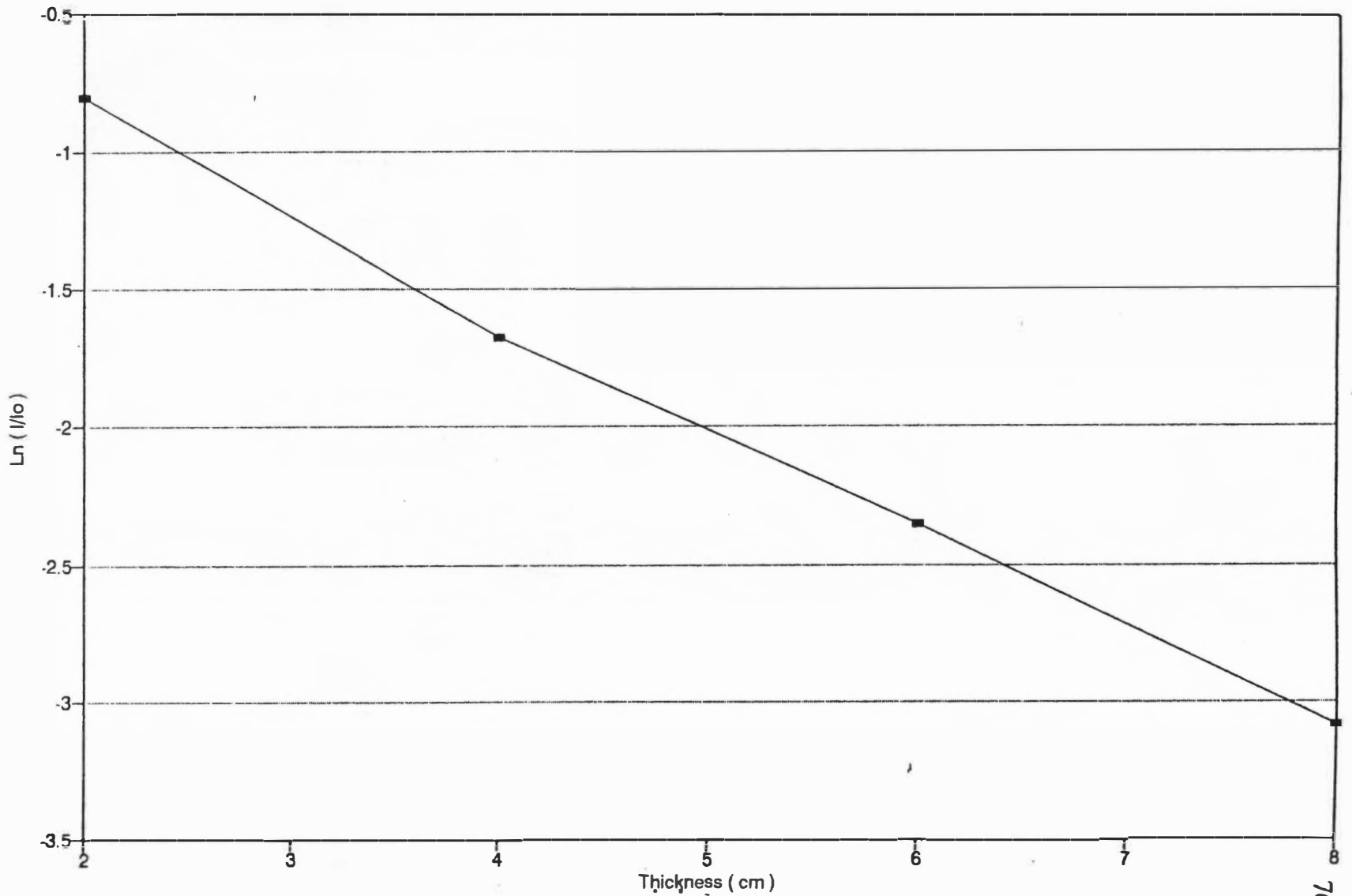


Figure 5.4 - Calibration test (four thicknesses of Oak).

mat. These two pieces of plywood, with the mat sandwiched between them, were secured together with drive screws. This sandwiched assembly was then trimmed into the four individual strips, representing the four different attenuation distances for initial study, i.e., 2, 4, 6, and 8 inch mat widths. In addition, a 12 inch mat width was also prepared.

Usual laboratory procedures for pressing mats were followed; 400<sup>0</sup>F platen temperature, 5 minute press cycle, approximately 30 seconds to position, and a de-gas step at the end of the cycle. For all mat widths, except the 12 inch mat, the radiation count rate was every two seconds. For the twelve inch mat width the count rate was every four seconds. Air counts were taken with no mats in the press for both hot and cold press conditions. No difference in air count data was found between cold and hot press conditions.

## RESULTS AND DISCUSSION

The intent of this initial experimentation was to validate the performance of the yoke-translation device and to demonstrate the concept of monitoring density in a horizontal plane within a mat during pressing. Figures 5.5 through 5.9 represent density data plotted for each of the mat widths (attenuated distances). Figures 5.10 through 5.14 show the same data after employing a transformation technique to smooth the data. These are the first known plots of *in-situ* density measurement during pressing ever recorded. Note that the time of stopping data logger varied among plots. For example, the graphs of density versus time in figures 5.5, 5.7, and 5.9 show that the data logger was stopped before the press opened and returned to "home" position. Whereas, in figure 5.6 and 5.8 the data logger was not stopped until after the press opened and returned to "home" position. In these later two graphs, the radiation source and detector went out of register with the completed particle board as the press opened. When this happened, the density dropped immediately to zero. The smoothed plots show this same effect.

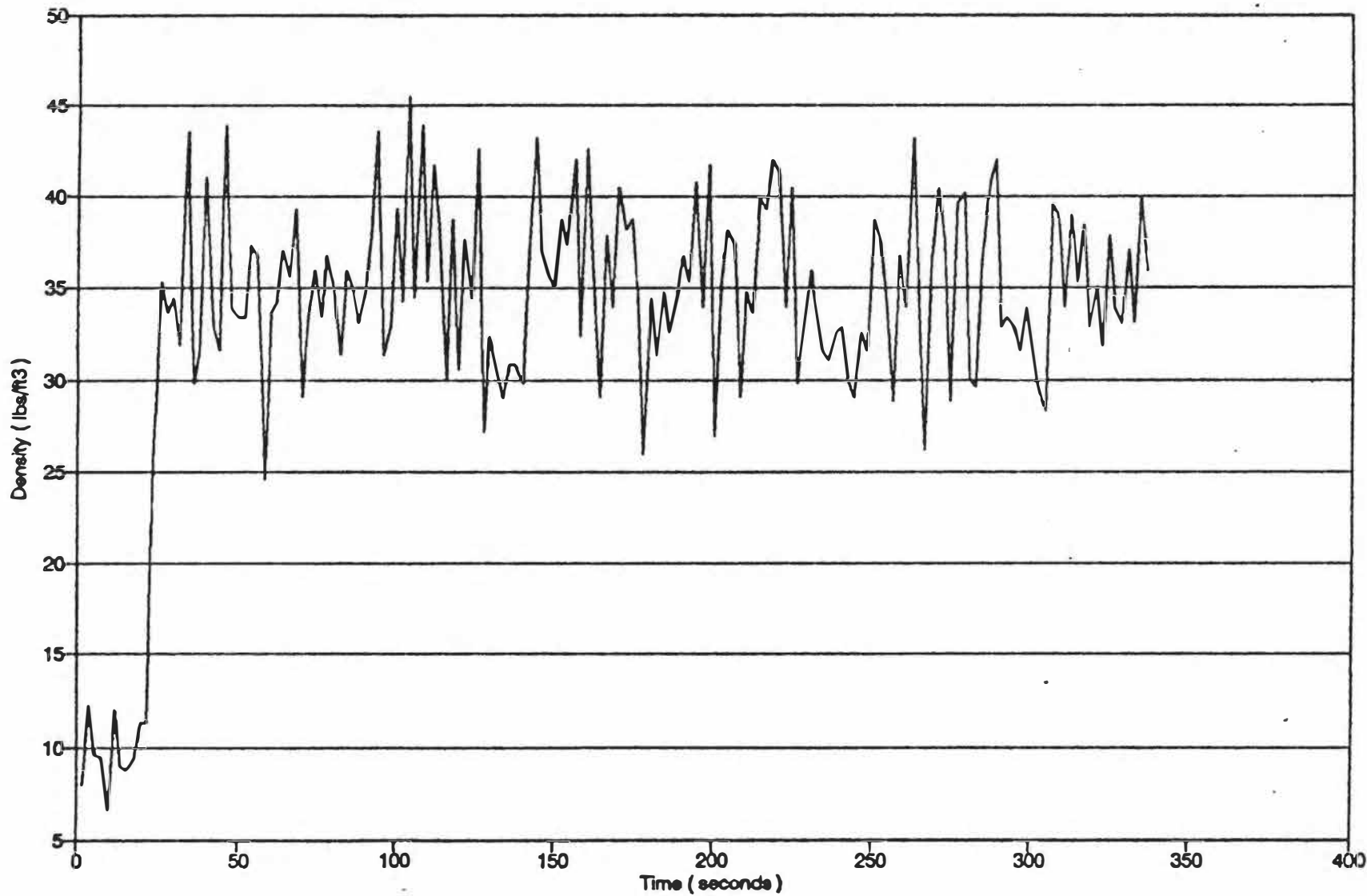


Figure 5.5 - Density during press cycle (sample:8 - width:2").

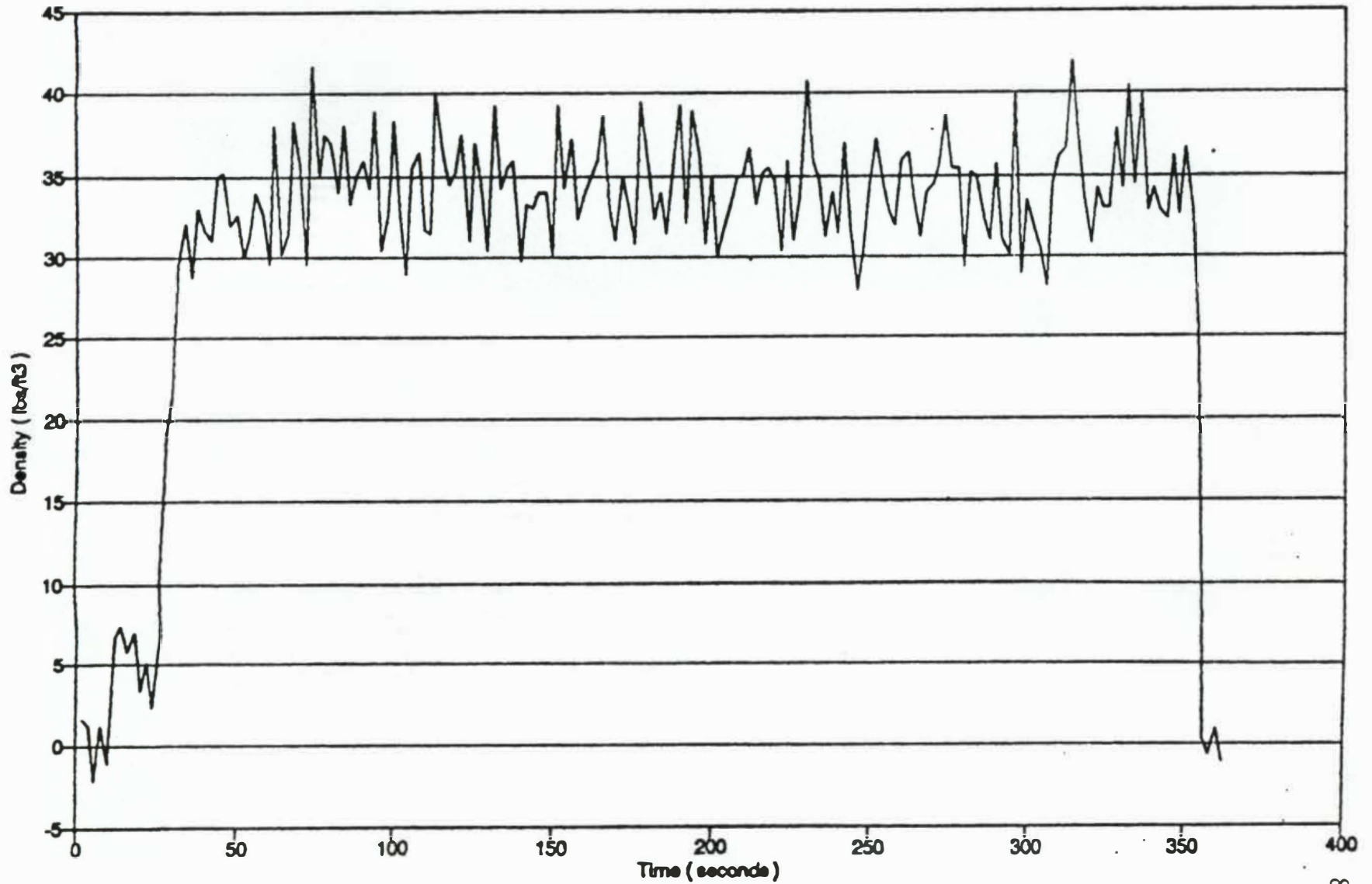


Figure 5.6 - Density during press cycle (sample:9 - width:4").

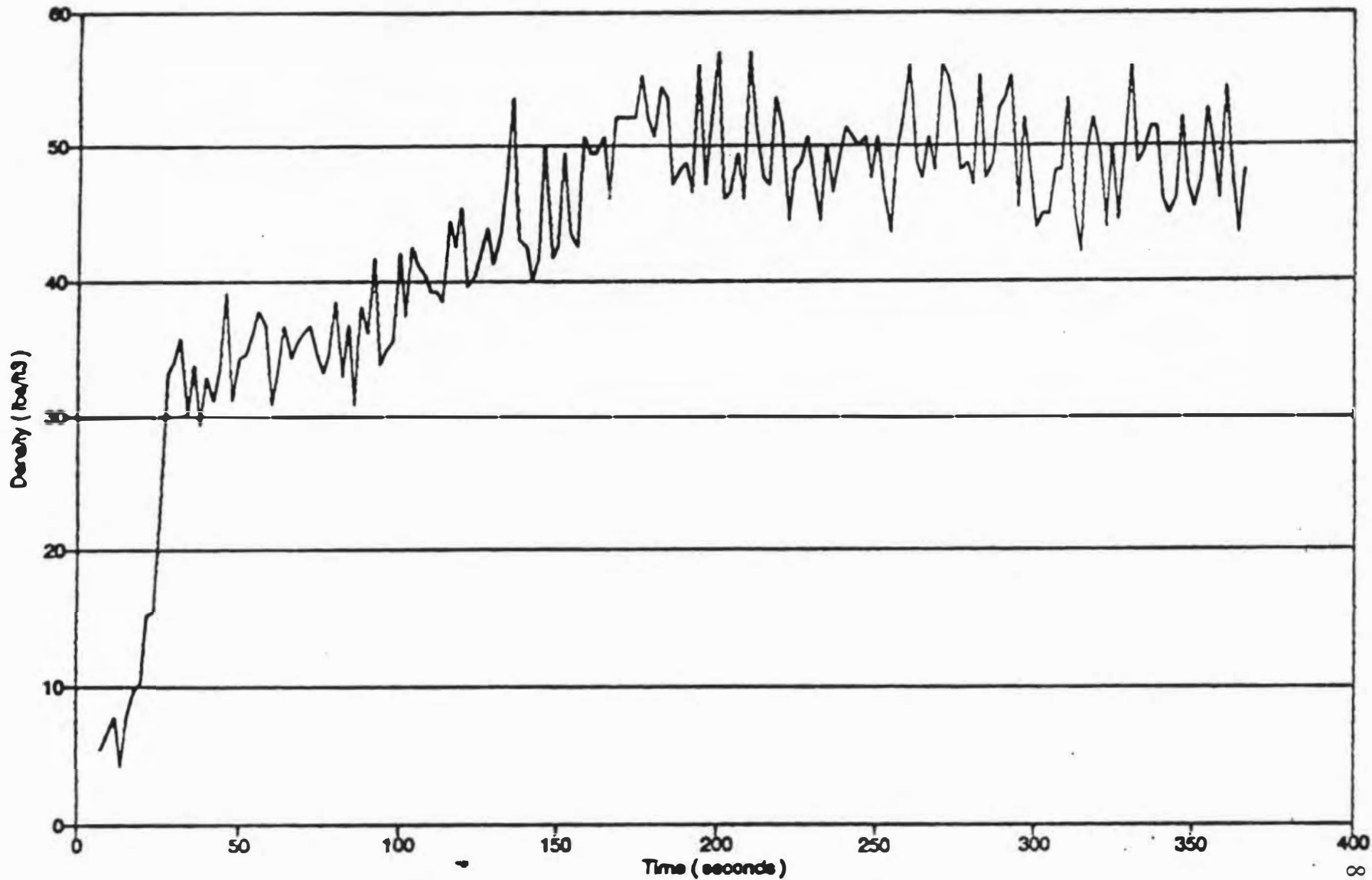


Figure 5.7 - Density during press cycle (sample:11 - width:6").

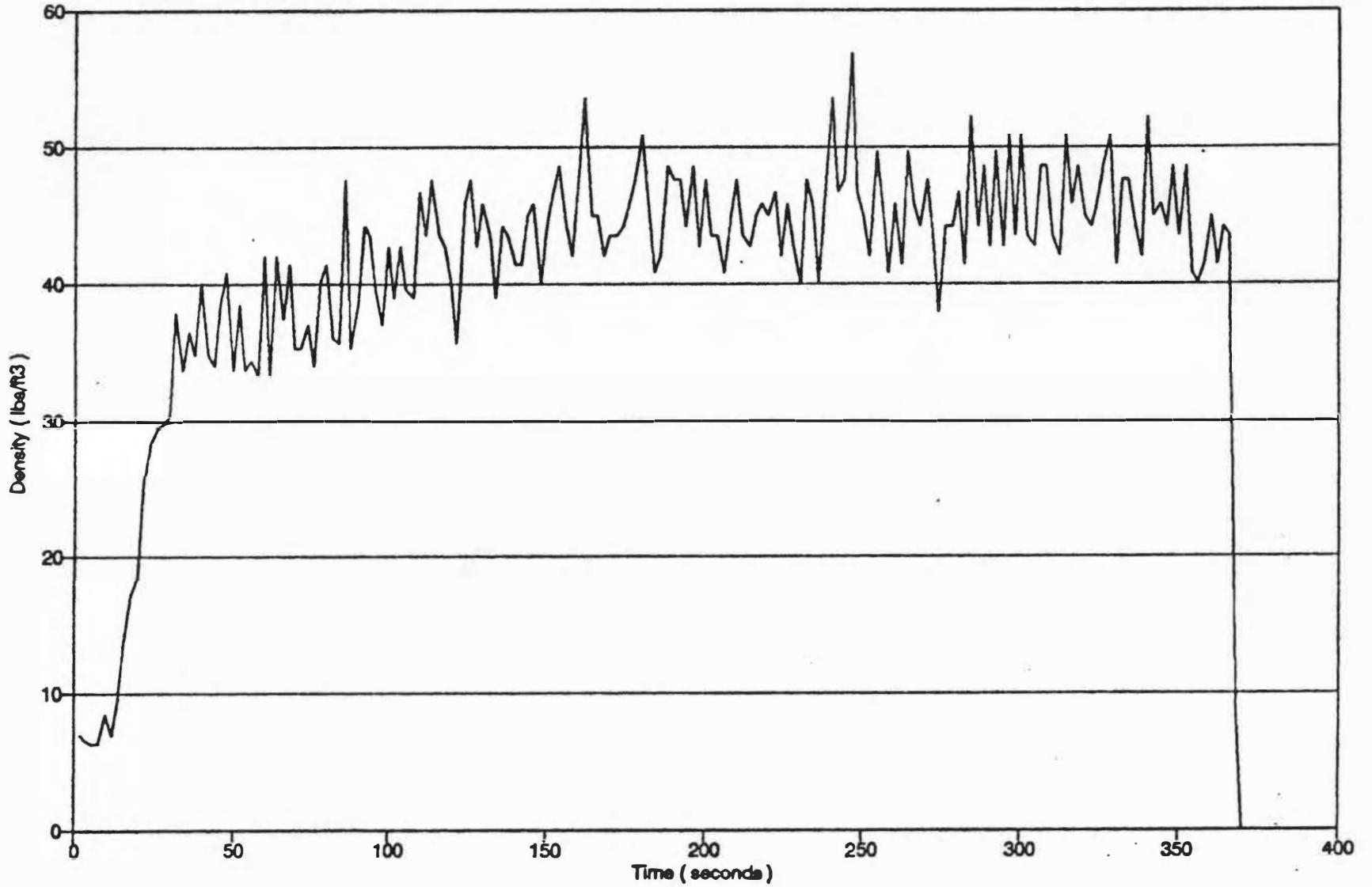


Figure 5.8 - Density during press cycle (sample:12 - width:8").

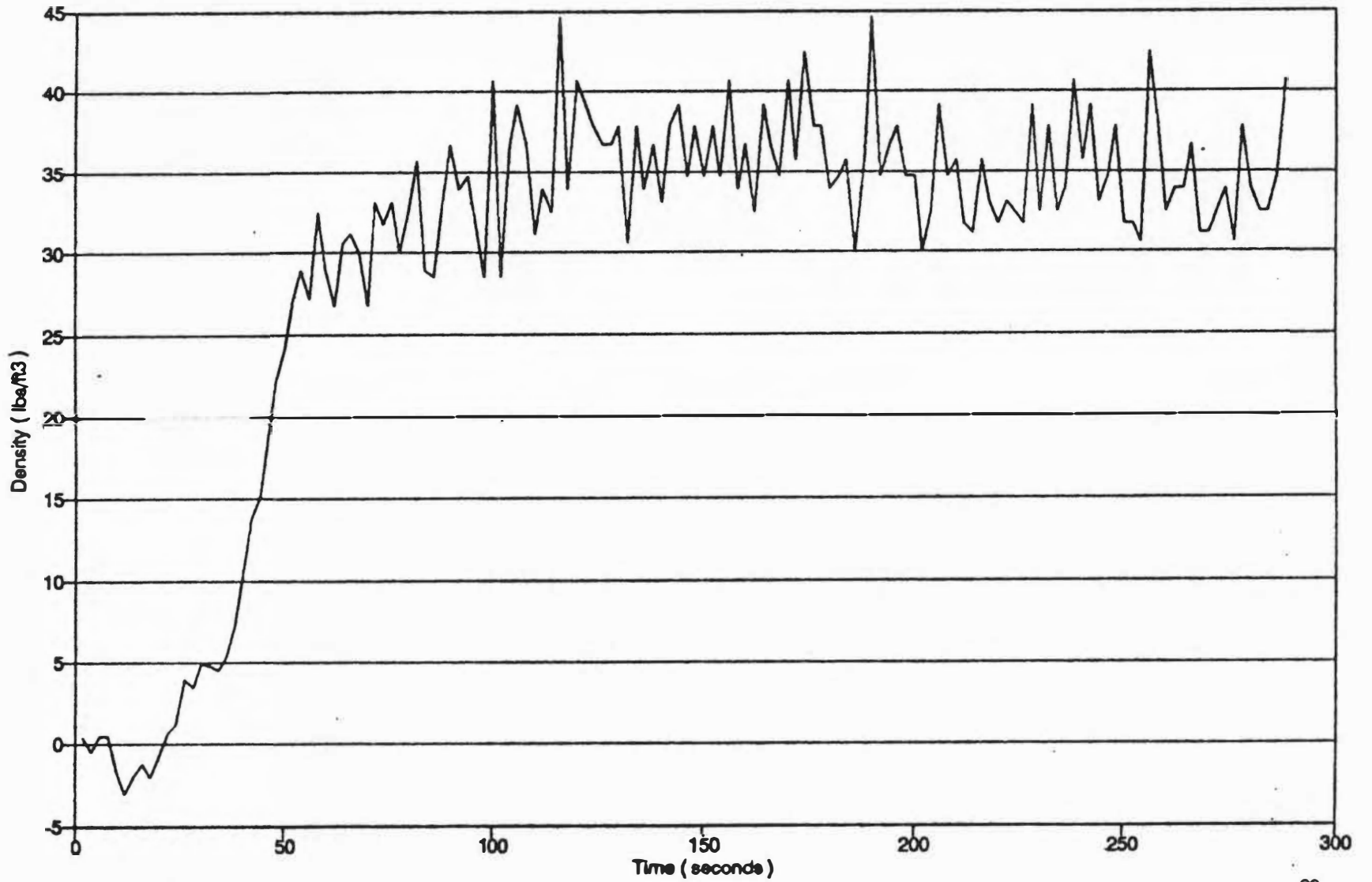


Figure 5.9 - Density during press cycle (sample:13 - width:12").

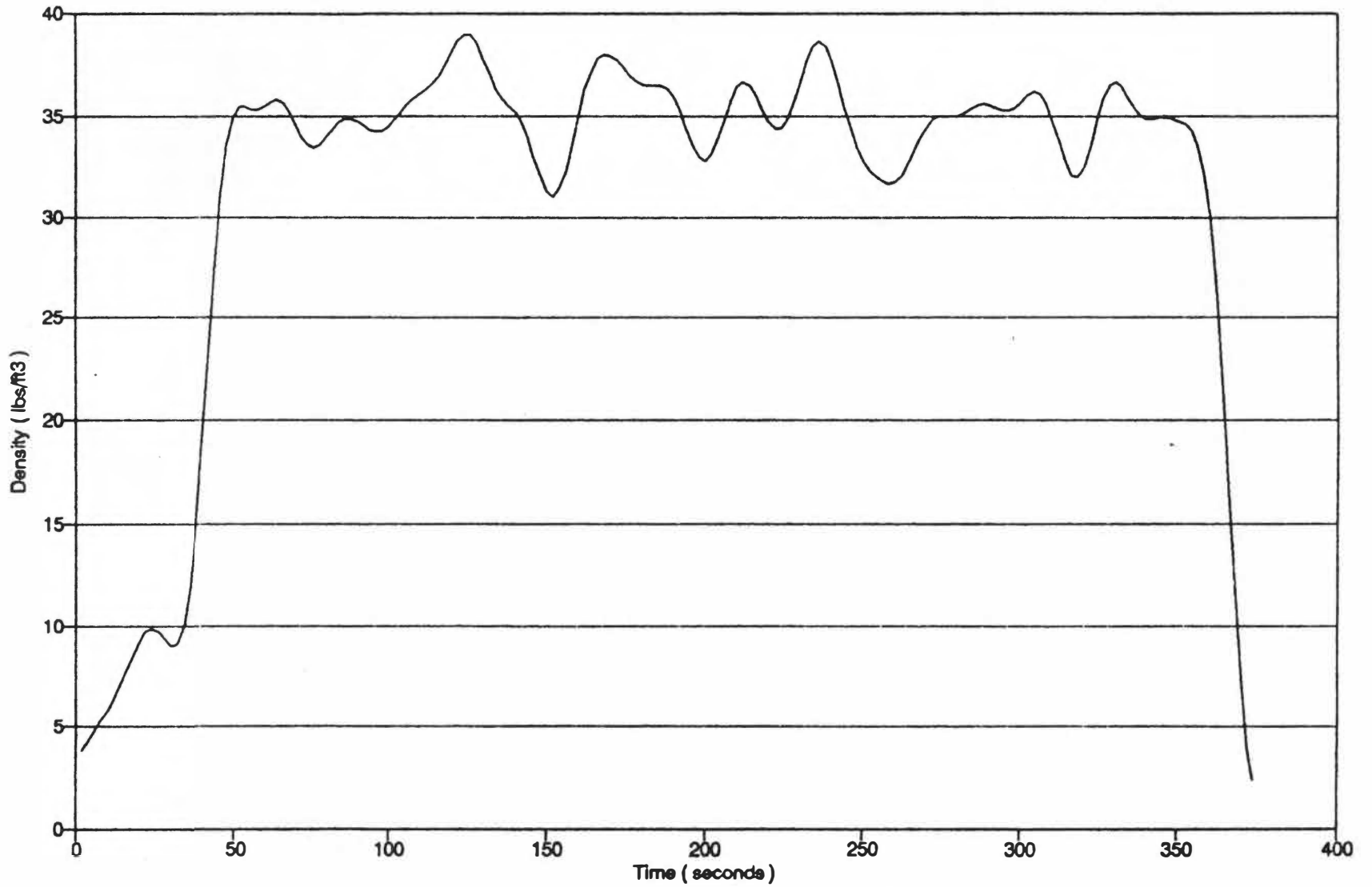


Figure 5.10 - Density during press cycle (sample:8 - width:2"), smoothed plot.

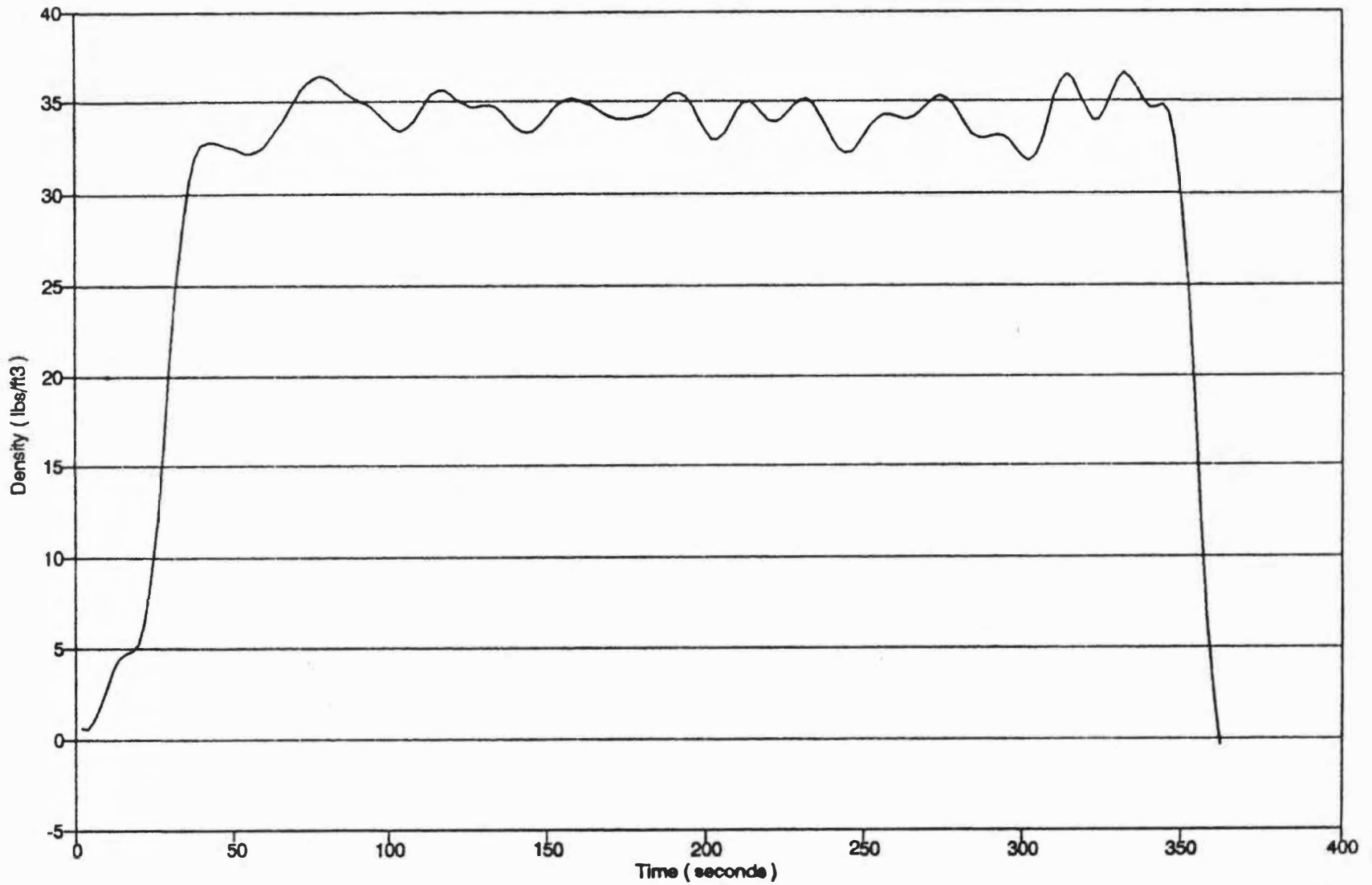


Figure 5.11 - Density during press cycle (sample:9 - width:4"), smoothed plot.

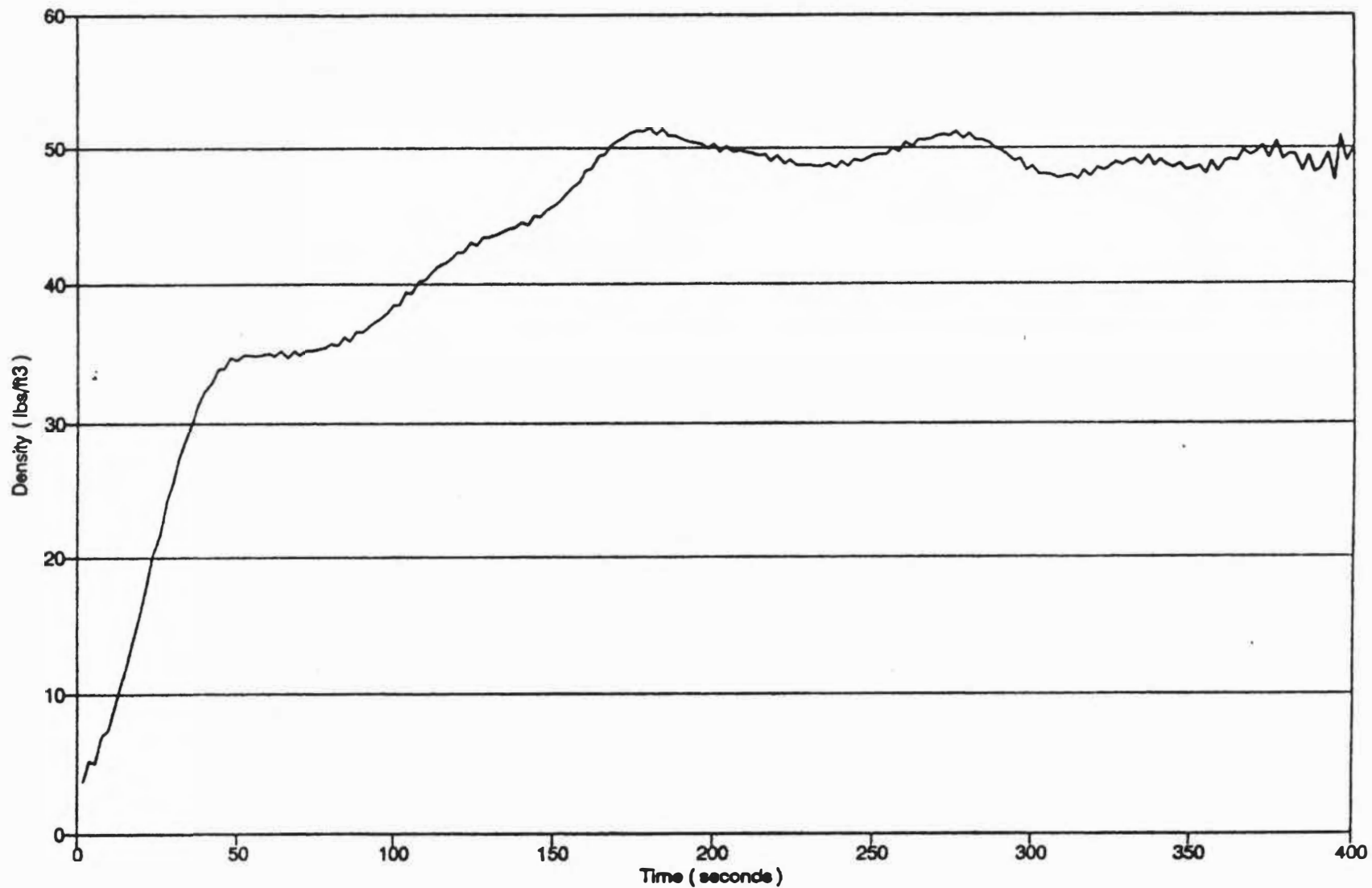


Figure 5.12 - Density during press cycle (sample:11 - width:6"), smoothed plot.

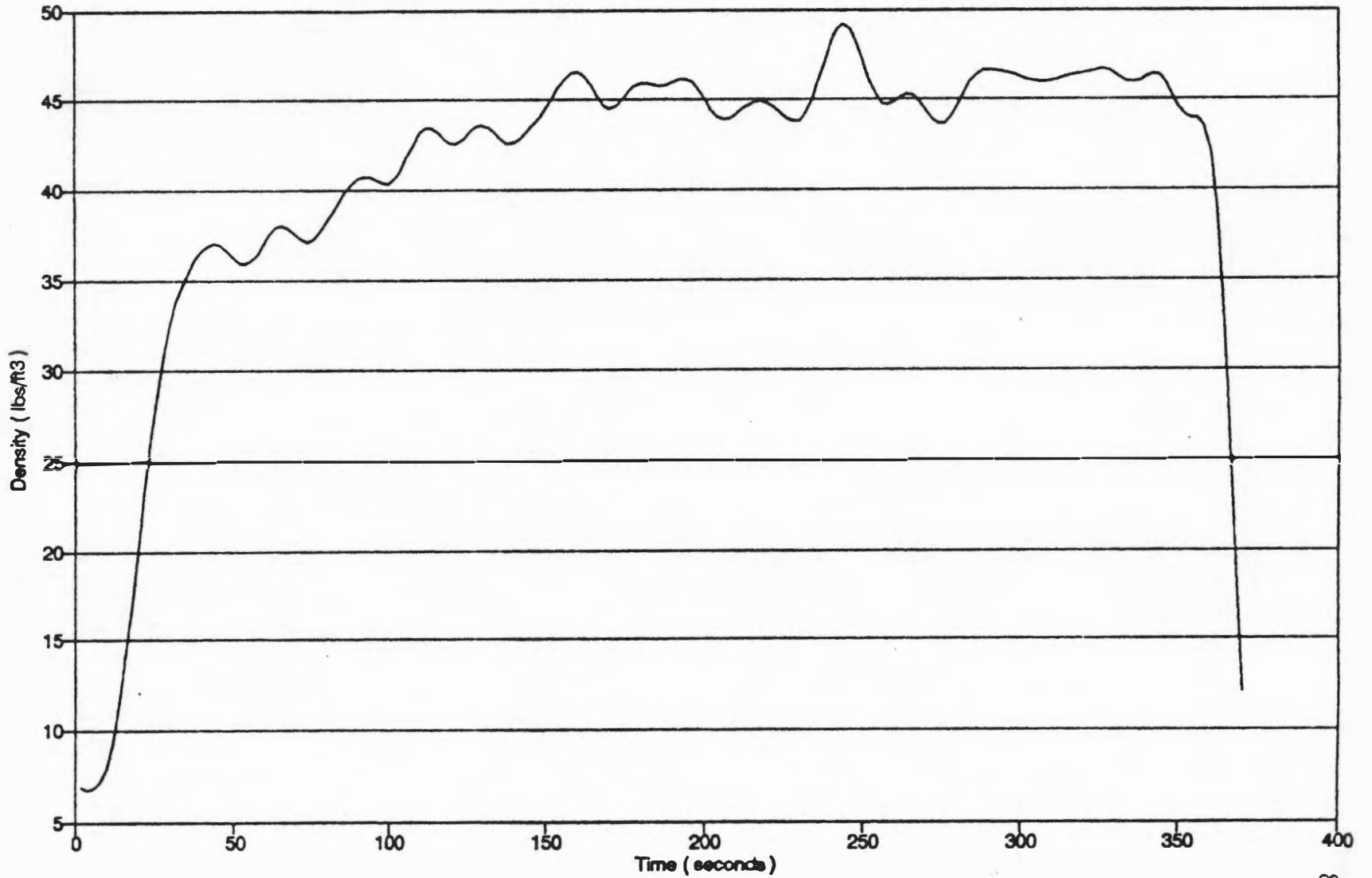


Figure 5.13 - Density during press cycle (sample:12 - width:8"), smoothed plot.

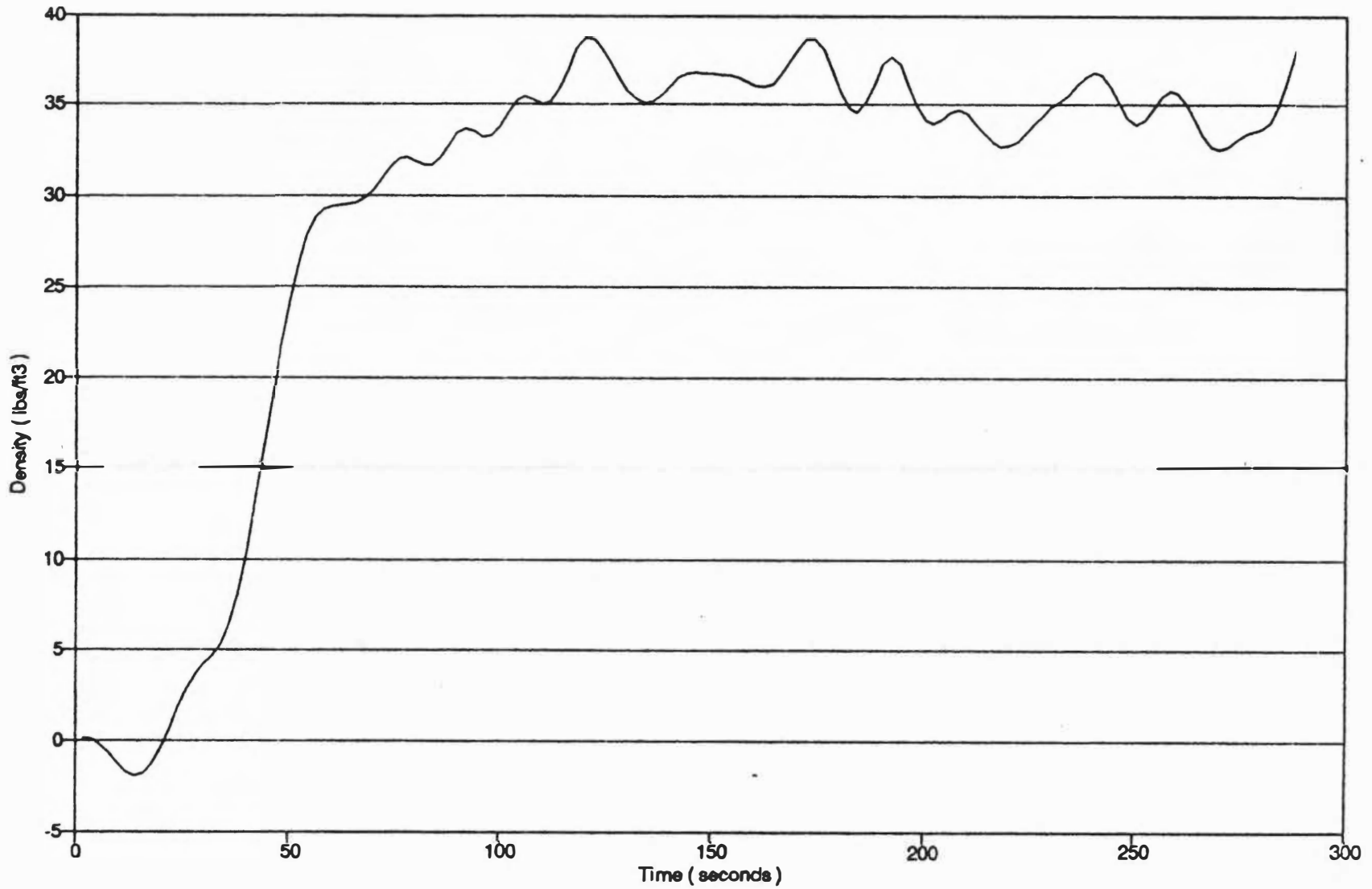


Figure 5.14 - Density during press cycle (sample:13 - width:12"), smoothed plot.

## CHAPTER 6

### CONCLUSION

The objective of this project was to design and fabricate a mechanical device to translate a radiation source and detector in fixed relative positions to the press opening distance. This objective was achieved; the yoke assemblies maintained relative positions, with good accuracy, during the evaluation of the device. During experimentation, the device performed at normal press operating temperatures (400 °F) with no variation in accuracy of the yoke-source-detector assembly position relative to press opening distance. Average relative difference (to a common reference plane) in position of the source and detector assembly for yoke #1 was 0.0026 inches. Position measurements made for source holders of yoke #1 and yoke #3 assure that position of yoke #2 is accurate, as all yoke assemblies are connected through the gear assemblies.

Initial experimentation with the Am<sup>241</sup> radiation source and detector attached to the device was promising; these were the first known measurements made of *in situ* density in a horizontal plane during pressing. The calibration of the radiation source positioned in the yoke assembly revealed a consistent linear attenuation coefficient for different sample widths. Plots of density with time during pressing were repeatable for samples of the same attenuation distance (width).

The main objective of this work was to design and develop the device for translating the radiation source and detector in concert with the moving press. With the operating accuracy of the device confirmed, future experimentation with this device should include consideration of a more appropriate source and detector to ensure ample radiation counts during the critical stage of press closure.

## **BIBLIOGRAPHY**

## BIBLIOGRAPHY

- Bolton, A. J., Humphrey, P. E. and P. K. Kavvouras P. 1989. The hot pressing of dry-formed wood-base composites. Part VI. The importance of stresses in the pressed mattress and their relevance to the minimisation of pressing time, and variability of board properties. *Holzforschung* 43:406-410.
- Cown, D. J. and Clement B. C. 1983. A wood densitometer using direct scanning with X-ray. *Wood Science & Technology* 17:91-99.
- Davis, W. C. T. 1989. The effect of furnish moisture content, press closure rate, and panel density on thickness swell and the vertical density profile of a mixed hardwood flakeboard. MS. Thesis Dept. of Forestry, Wildlife and Fisheries. University of Tennessee. Knoxville, Tennessee. 118 pp.
- Deutschman, A. D., Michels, W. J. and Wilson, C. E. 1975. *Machine Design Theory and Practice*. Macmillian Publishing Co., Inc. New York. 931 pp.
- Fritton, D. D. 1969. Resolving time, mass absorption coefficient and water content with gamma-ray attenuation. *Soil Science Society of American Proc.* 33:651-654.
- Gardner, W. H., Campbell, G. S. and Calssendorff, C. 1976. Systematic and random errors in dual gamma energy soil bulk density and water content measurements. *Soil Science of American Proc.* 36:393-397.
- Geimer, R. L., Montrey, H. M. and Lehmann, W. 1975. Effects of layer characteristics on the properties of three-layer particleboards. *Forest Products Journal* 25(3):19-29.
- Goldanskii, V. I., Kutsenko, A. V. and Podggoretskii, V. I. 1962. *Counting Statistic of Nuclear Particles*. Hindistan Publishing Corporation. Delhi-6. India. 478 pp.
- Harless, T. E. G., Wagner, F. G. , Short, P. H, Seale, R. D. , Mitchell P. H. and Ladd, D. S. 1987. A model to predict the density profile of particleboard. *Wood and Fiber Science* 19(1):81-92.
- Hoag, M. L. and Krahmer. 1991. Polychromatic X-ray attenuation characteristics and wood densitometry application. *Wood and Fiber Science* 23(1):23-31.

- Hoag, M. and McKimmy, M. D. 1988. Direct scanning x-ray densitometry of thin wood sections. *Forest Products Journal* 38(1):23-26.
- Humphrey, P. E. 1990. Some physical transformations that occur during the cure of noseting adhesive-to-wood. Wood adhesives. *Proceedings of a symposium sponsored by USDA Forest Service, Forest Products Laboratory and Forest Products Research Society.*
- Humphrey, P. E. 1988. Moisture movement and its implications during the manufacture of wood-based composites. *Executive Summaries. 43rd Annual Meeting. Forest Products Research Society.*
- Juvinall, R. C. 1983. *Fundamentals of Machine Component Design.* John Willey & Sons. New York. 761 pp.
- Kamke, F. A. and Casey, L. J. 1988. Fundamentals of flakeboard manufacture: internal-mat condition. *Forest Products Journal* 38(6):38-44.
- Kamke, F. A. and Casey, L. J. 1988. Gas pressure and temperature in the mat during flakeboard manufacture. *Forest Products Journal* 38(3):41-43.
- Kamke F. A. and Wolcott M.P. 1991. Fundamentals of flakeboard manufacture: wood-moisture relationship. *Wood Science and Technology* 25:57-71.
- Kayihan F. and Johnson, J. A. 1983. Heat and moisture movement in wood composite materials during pressing operation - a simplified model. *Numerical Methods in Heat Transfer. Volume II.* John Wiley & Sons Ltd. New York. 536 pp.
- Kelly, M. W. 1977. Critical literature review of relationships between processing parameters and physical properties of particleboard. *General Technical Report FPL-10.* USDA Forest Products Laboratory. 65 pp.
- Korff, S. A. 1955. *Electron and Nuclear Counters, Theory and Use.* D. Van Nostrand Company, Inc. New York. 363 pp.
- Lapp, R. E. and Andrews, H. L. 1948. *Nuclear Radiation Physics.* Prentice-Hall, Inc. New York. 483 pp.
- Laufenberg, T. L. 1986. Using gamma radiation to measure density gradients in reconstituted wood product. *Forest Products Journal* 36(2):59-62.

- Liebhafsky, H. A., Pfeiffer, H. G., Winslow, E. H. and Zeman P. D. 1960. *X-Ray Absorption and Emission in Analytical Chemistry*. John Wiley & Sons, Inc. New York. 357 pp.
- Linear Motion Technology Guide*. 1991. Thompson Industries Inc. Port Washington, NY 11050.
- Liu, C. J., Olson, R. J, Tian, Y. and Shen Q. 1988. Theoretical wood densitometry: I. Mass attenuation equations and wood density models. *Wood and Fiber Science* 20(1):22-34.
- Liu, C. J., Olson, R. J, Tian, Y. and Shen Q. 1988. Theoretical wood densitometry: II. Optimal X-ray energy for wood density measurement. *Wood and Fiber Science* 20(2):187-196.
- Loos, W. E. 1961. The relationship between gamma-ray absorption and wood moisture content and density. *Forest Products Journal* 11(3):145-149.
- Loos, W. E. 1965. Determining moisture content and density of wood by nuclear radiation techniques. *Forest Products Journal* 15 (2):102-106.
- McFarland, D.L. and P. M. Winistorfer. 1991. Computer automation of a laboratory hot press. IN: *Proceedings of 45th Annual Meeting Forest Products Research Society*. New Orleans. LA. June 1991.
- Moschler, W. W. Jr. and Dougal E. F. 1988. Calibration Procedure for a direct scanning densitometer using gamma radiation. *Wood and Fiber Science* 20(3):297-303.
- Moschler, W. W., Jr. and Winistorfer, P. M. 1990. Direct scanning densitometry: an effect of sample heterogeneity and aperture area. *Wood and Fiber Science* 22(1):31-38.
- Near, W. T. and Basset, K. 1968. X-ray determination and use of surface-to-surface density profile in Fiberboard. *Forest Products Journal* 18(1):73-74.
- Price, W. J. 1958. *Nuclear Radiation Detection*. McGraw-Hill Book Company. New York. 430 pp.
- Ross, S. M. 1987. *Introduction to Probability and Statistics for Engineers and Scientist*. John Wiley & Sons. New York. 491 pp.

- SAS Users Guide: Statistics*. 1985. Statistical Analysis System Institute Inc. Cary, North Carolina.
- Simpson, W. T. 1973. Predicting equilibrium moisture content in wood by mathematical model. *Wood Fiber* 5:41-49.
- Steiner, P. R., Chow, S. and Nguyen D. 1978. Improving mill waferboard properties by X-ray-densitometer evaluation methods. *Forest Products Journal* 28(12):33-34.
- Strickler, M. D. 1959. Properties of Douglas-fir flakeboard. *Forest Products Journal* 9(6):203-215.
- Smith, D. C. 1982. Waferboard press closing strategies. *Forest Products Journal* 32(3):40-45.
- Suchsland, O. 1962. The density distribution in flake boards. *Quarterly Bulletin of Michigan Ag. Exp. Station*. M. S. U. Press 45(1): 104-121.
- Suchsland, O. and Woodson, G. 1975. Effect of press cycle variables on density gradient of medium-density fiberboard. In: *Eighth Washington State University Symposium on Particleboard*. T. M. Maloney Ed. Pullman, Washington.
- The Torrington Company Service Catalog*. 1988. The Torrington Company. Torrington, Connecticut.
- Woodson, G. E. 1976. Effects of bark, density profile, and resin content on medium-density fiberboards from Southern Hardwood. *Forest Products Journal* 26(2):39-42.
- Winistorfer, P. M., Davis, W. C. and Moschler, W. W. Jr. 1986. A direct scanning densitometer to measure density profiles in wood composite products. *Forest Products Journal* 36(11/12):82-86.

## VITA

Estevao Vicente Cavalcanti Monteiro de Paula was born in the city of Manaus, in the state of Amazonas, Brazil, on september 30. 1951. His education, from elementary school to college was obtained in the local public schools in the city of Manaus. In 1977, he graduated from the University of Amazonas with a Civil Engineer degree. In 1977 to 1981 Estevao worked as an engineer at Modiesel S.A. Industrial e Comercio. In 1982 he concluded his master's program in Structural Engineering at the Sao Carlos Engineering School of the University of Sao Paulo. From 1982 to this date, Estevao has worked as a researcher at National Institute for Research in the Amazon (INPA), in Manaus. During his tenure at INPA, Estevao has occupied several technical and administrative position including that of Head of the Wood Engineering Division, Head of the Construction Technical Office and Director of the Forest Products Research Center. In 1989, Estevao initiated his doctoral work at University of Tennessee in Knoxville. He concluded his work with the presentation of this dissertation on August, 15. 1992.